Probing Galaxy Clusters by Combining Strong and Weak Gravitational Lensing in the JWST Era:
Mass Reconstruction of Abell 2744

Sangjun Cha (Yonsei University)

in collaboration with Kim HyeongHan, Zachary P. Scofield, Hyungjin Joo, and M. James Jee

The 11th KIAS Workshop on Cosmology and Structure Formation @ Gyeongju



YOUNG

Yonsei Observable UNiverse Group

arXiv:2308.14805
Published in ApJ

Abell 2744 - Pandora's Cluster

Dissociative Merger & Offsets & Interloper

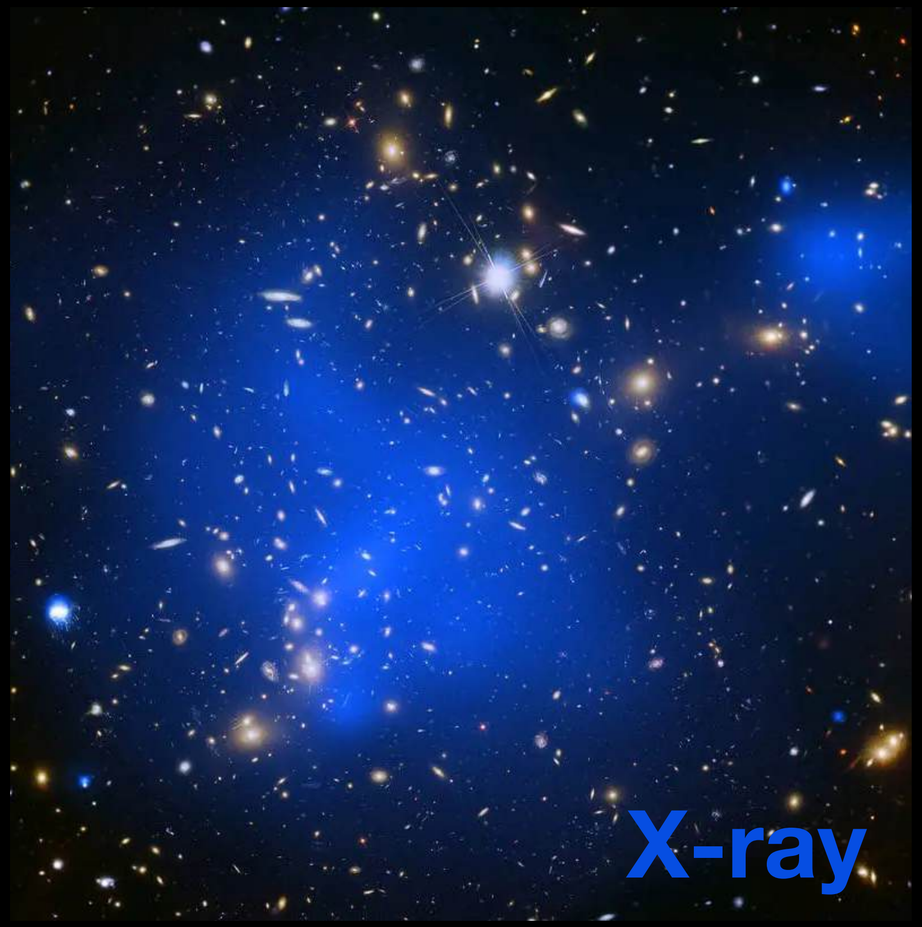
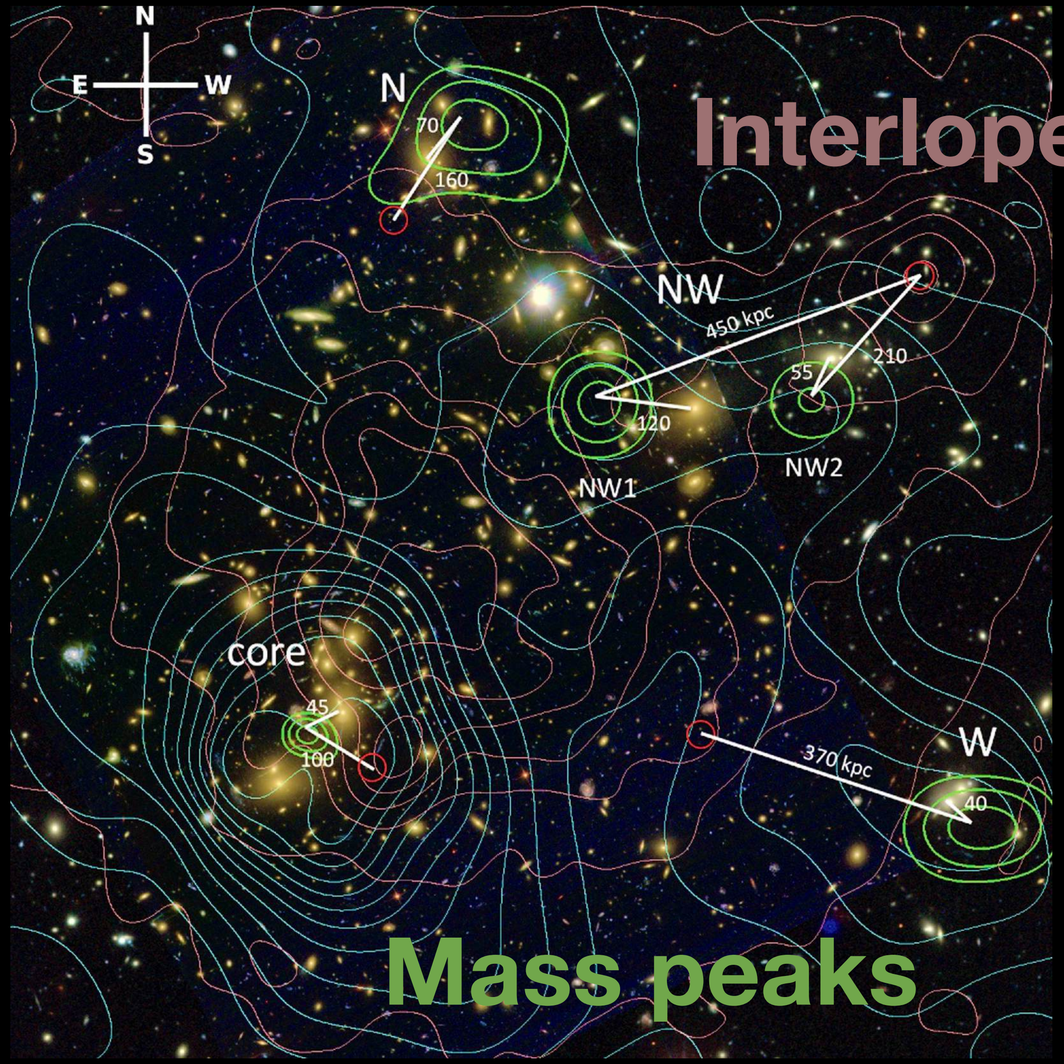
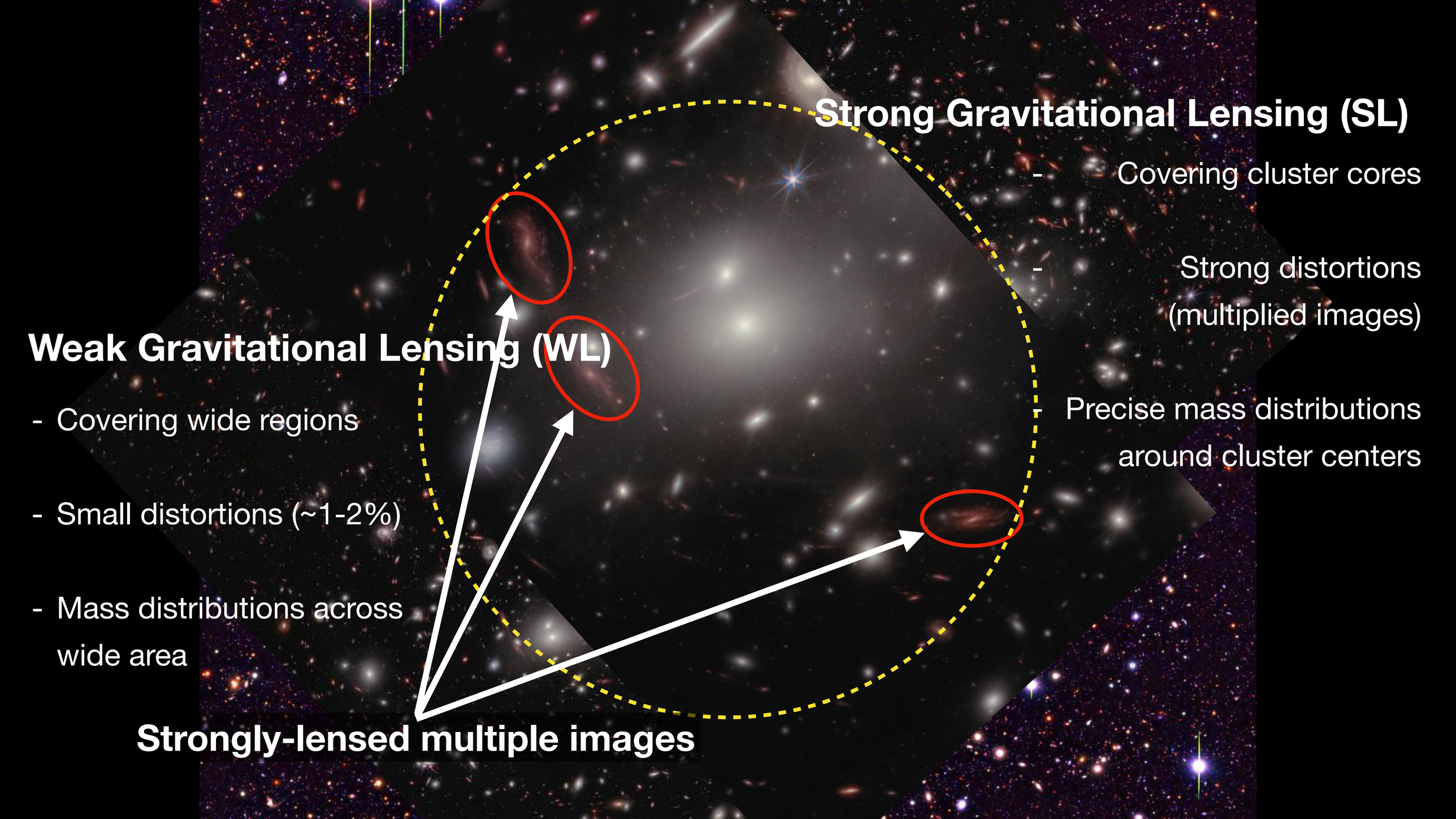


Image Credit: NASA/CXC/STScI

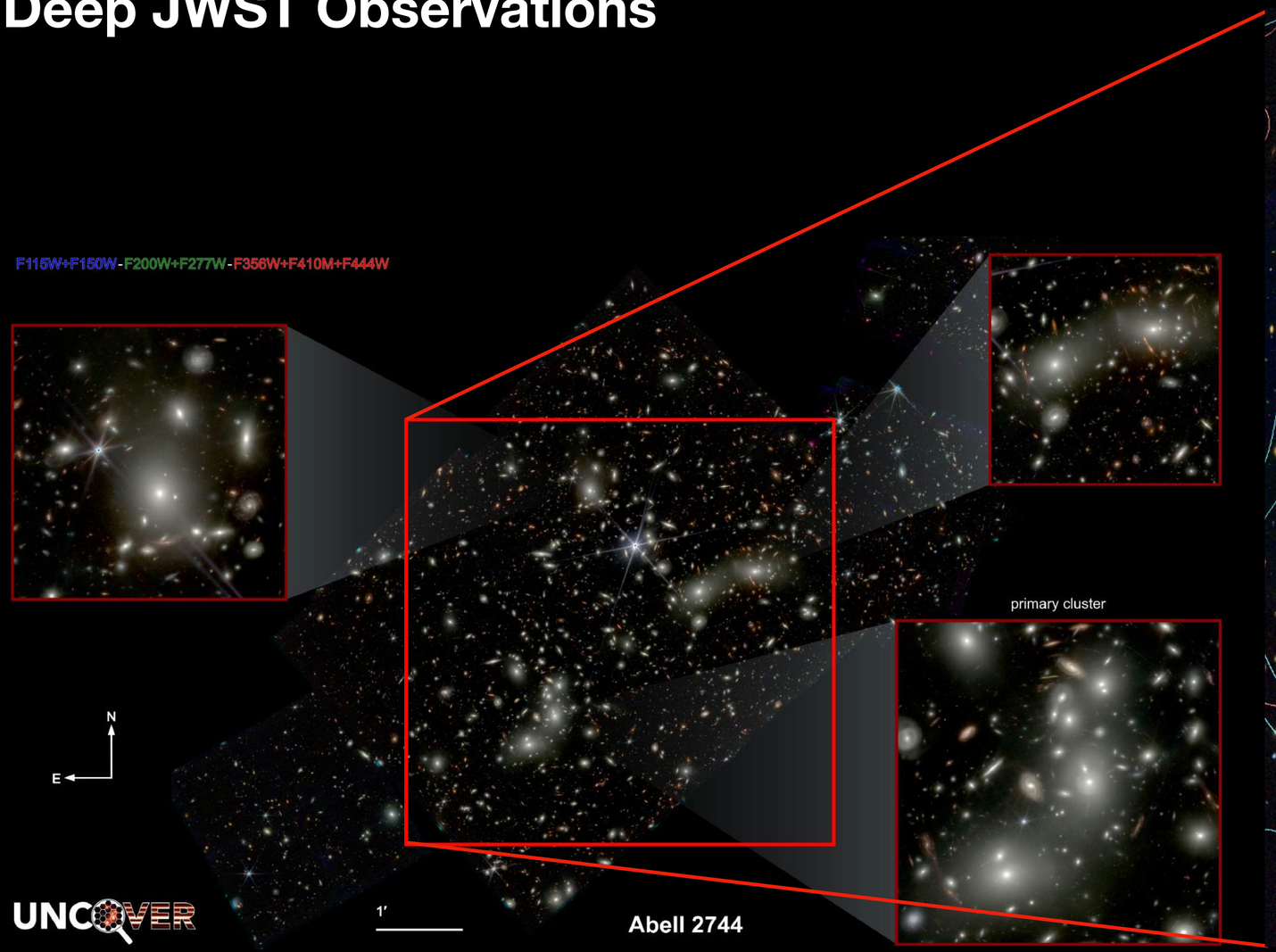


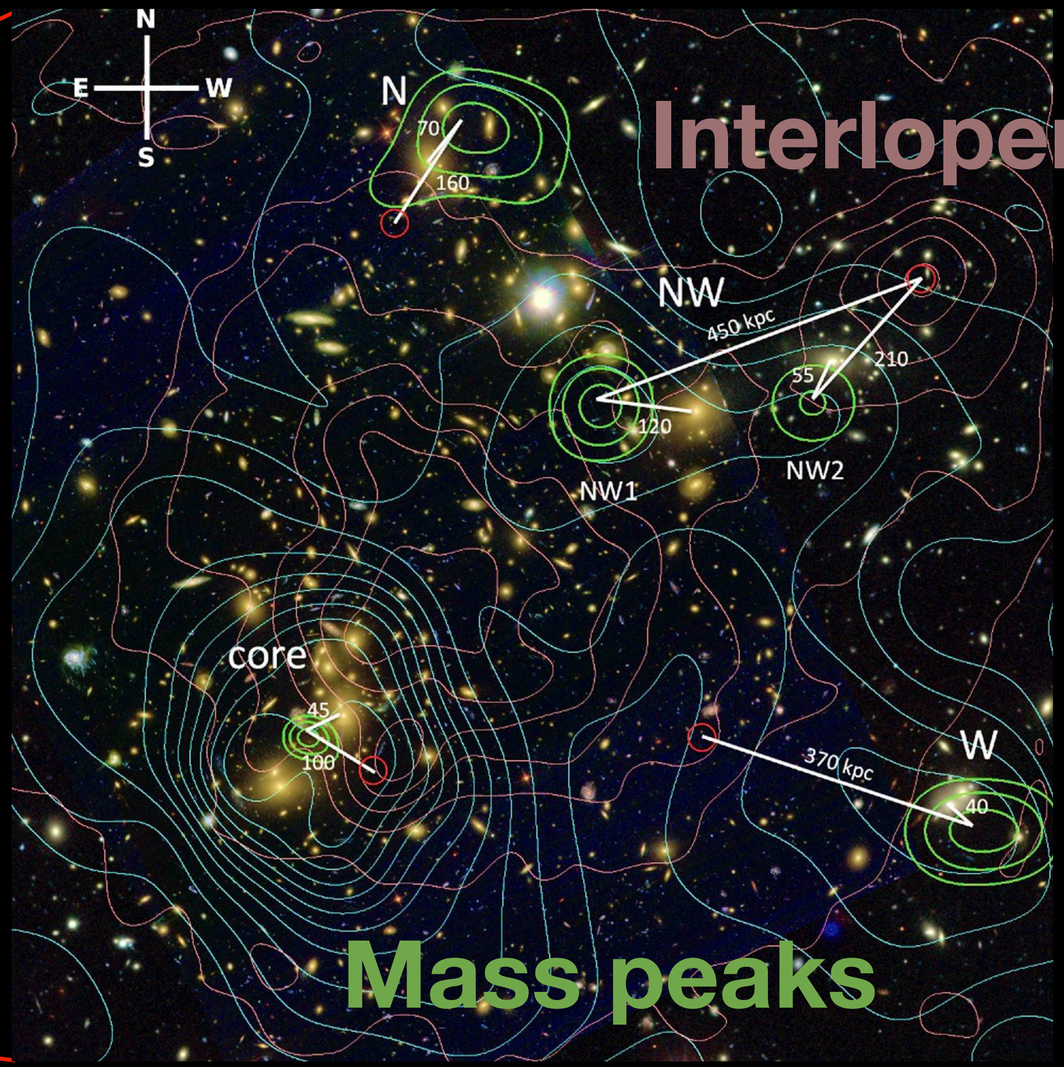
Merten et al. (2011); arXiv:1103.2772


Strong Gravitational Lensing (SL)
- Covering cluster cores
- Strong distortions (multiplied images)
- Precise mass distributions around cluster centers
Weak Gravitational Lensing (WL)
- Covering wide regions
- Small distortions (~1-2%)
- Mass distributions across wide area
Strongly-lensed multiple images

Abell 2744 - Pandora Cluster

Deep JWST Observations



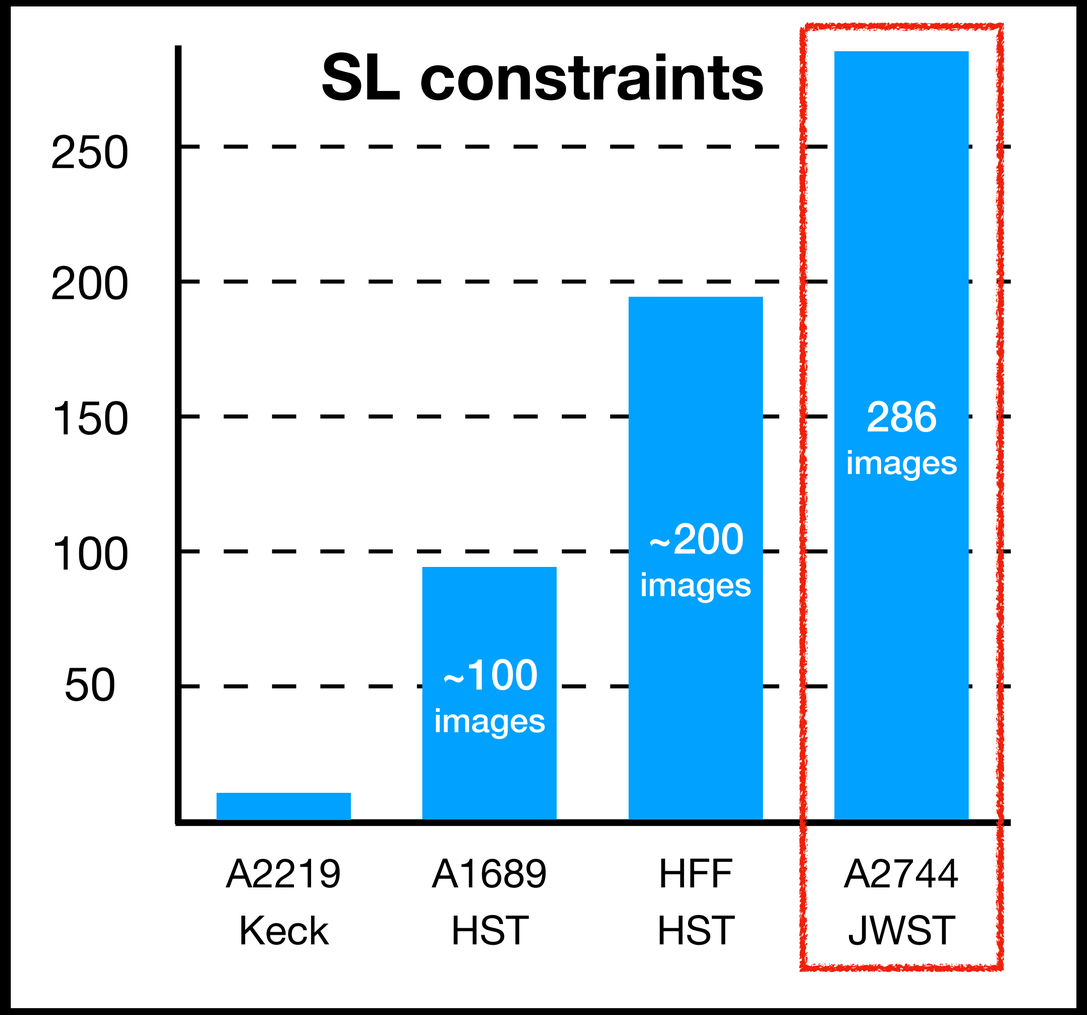


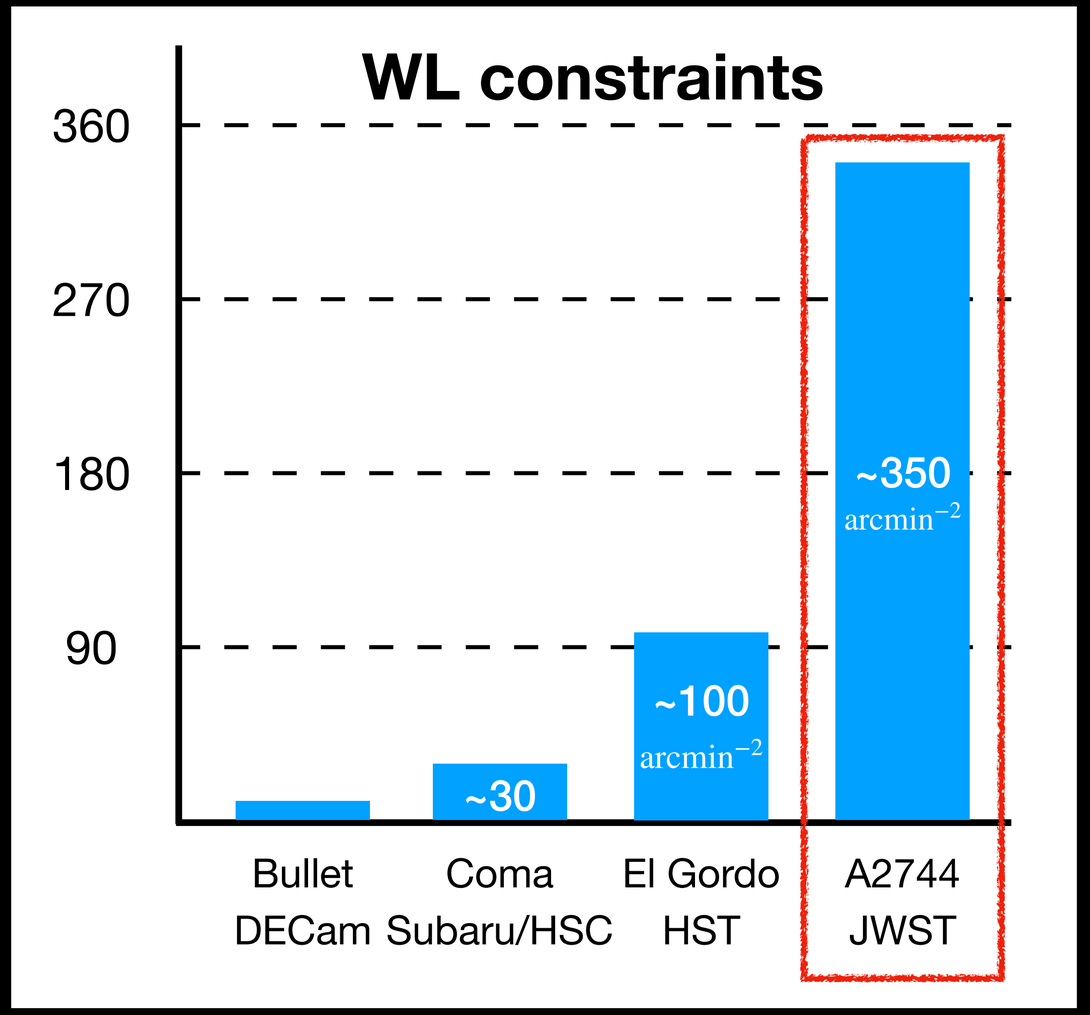
Bezanson et al. (2022); arXiv:2212.04026

Merten et al. (2011); arXiv:1103.2772

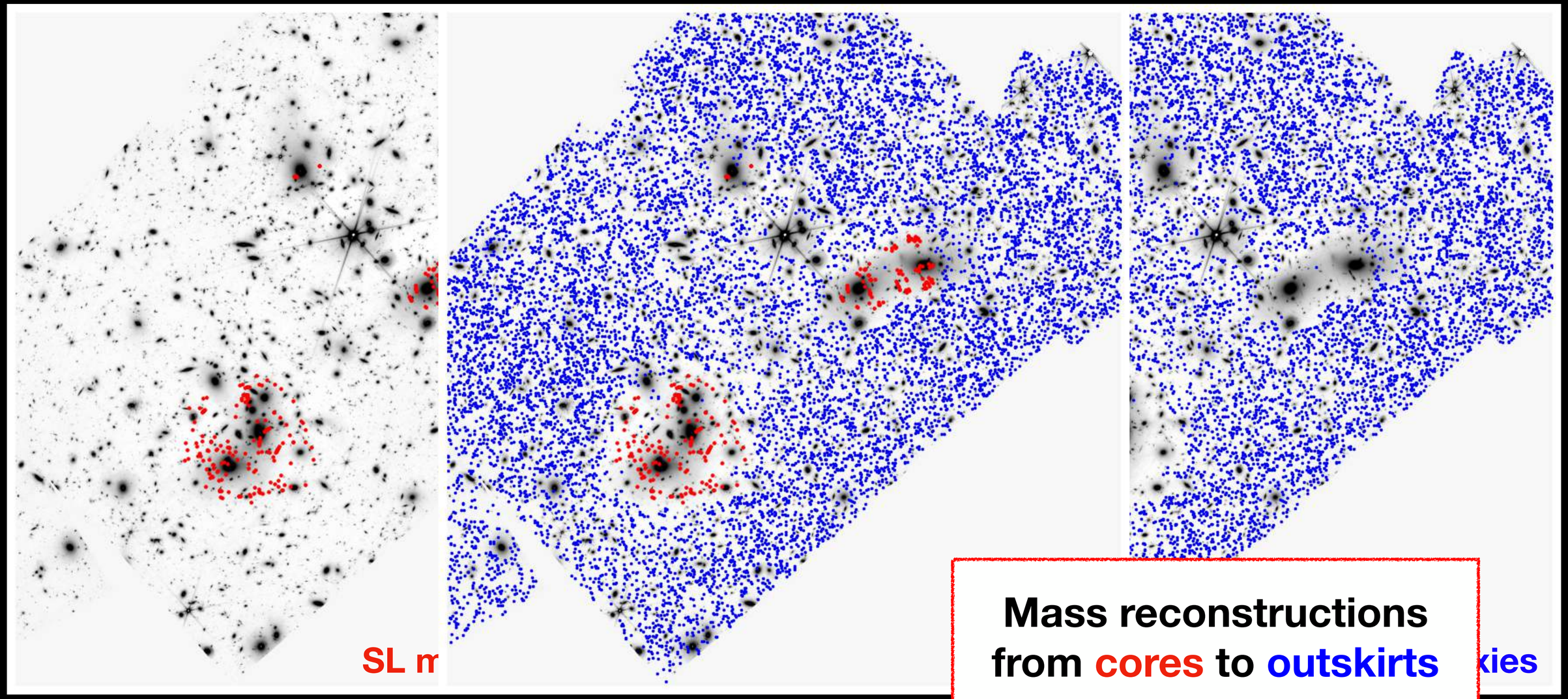
Largest Dataset for Modeling

Deep JWST Observations



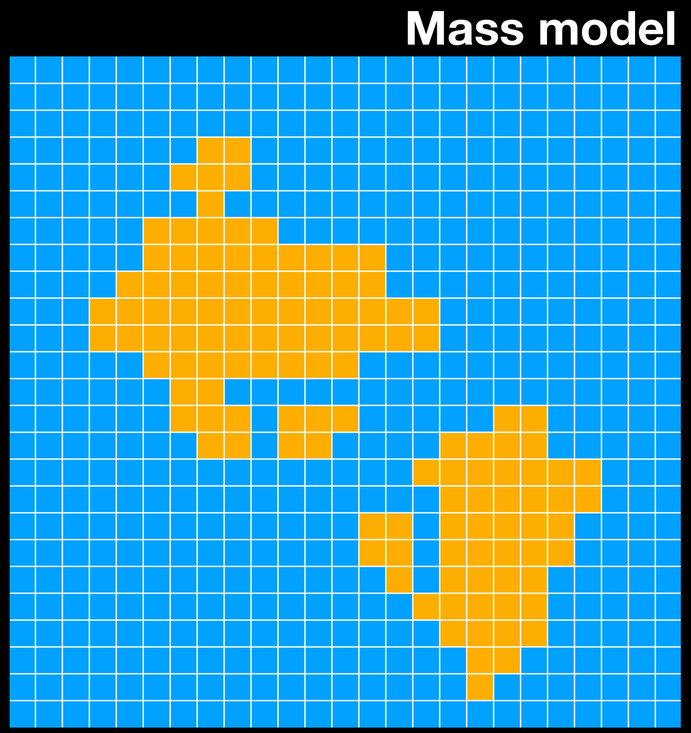


Combining WL and SL



Mass reconstructions from cores to outskirts

MAximum-entropy ReconStruction (MARS)



- **MARS is a grid-based, free-form method.**

- Does not use positional information of cluster member galaxies.

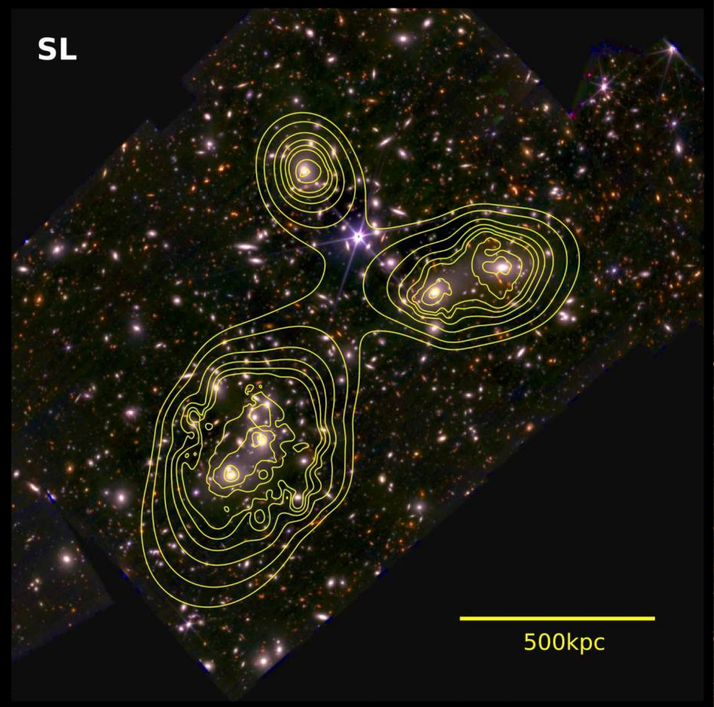
- Does not require assumptions for mass distributions.

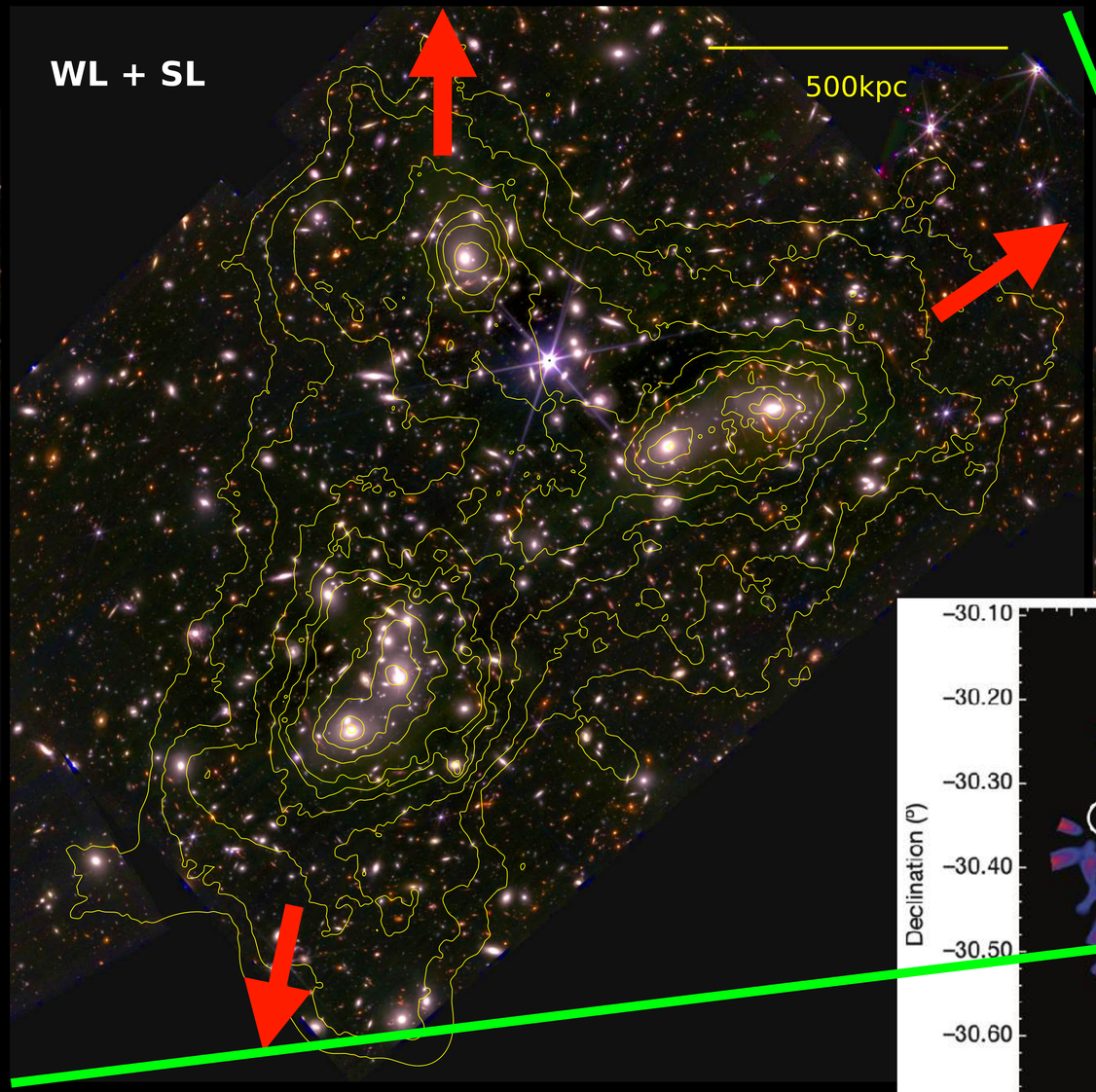
➡ Model-independent mass maps

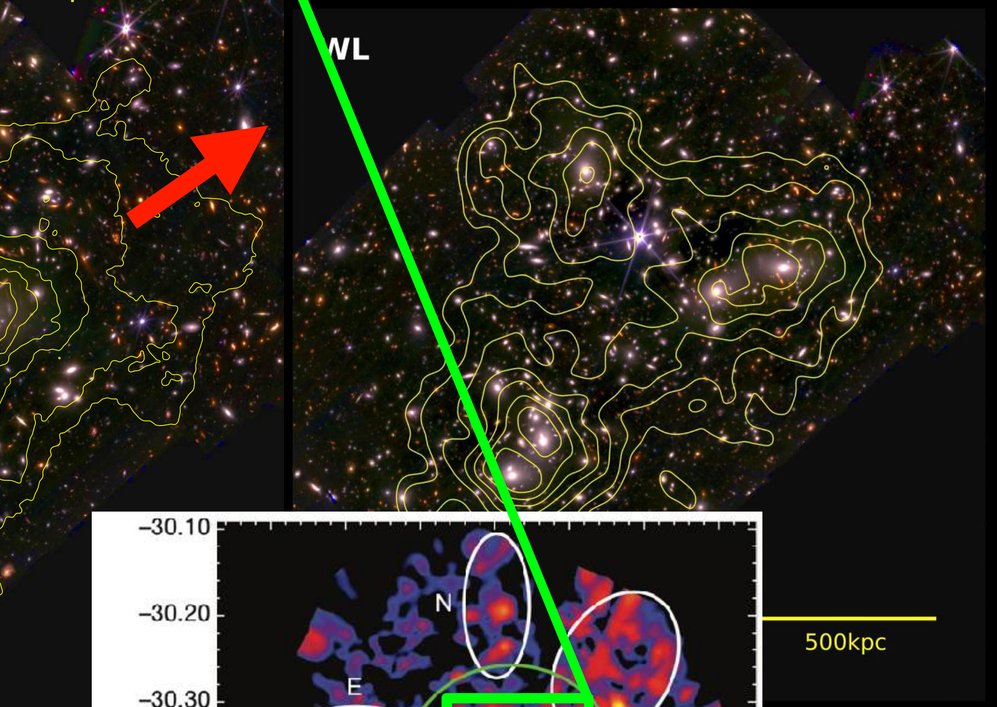
Please see my poster for more details about MARS!

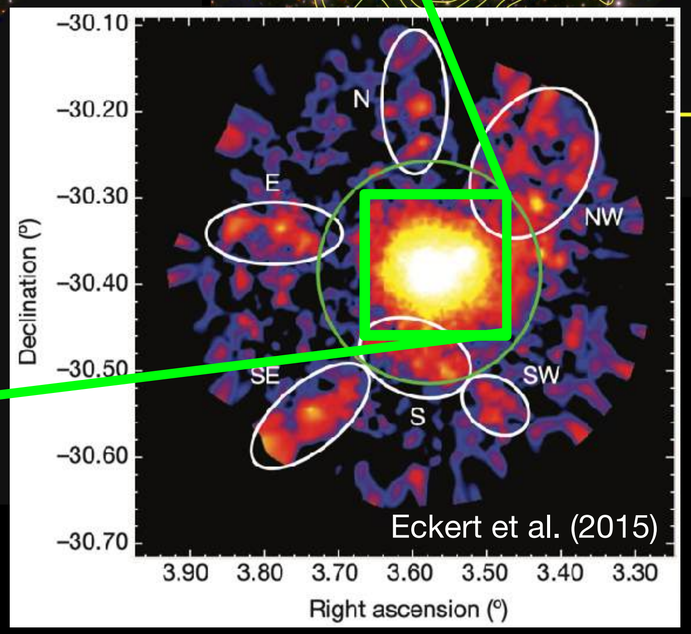
Cha & Jee (2022); arXiv:2202.10489

Mass Contours from MARS





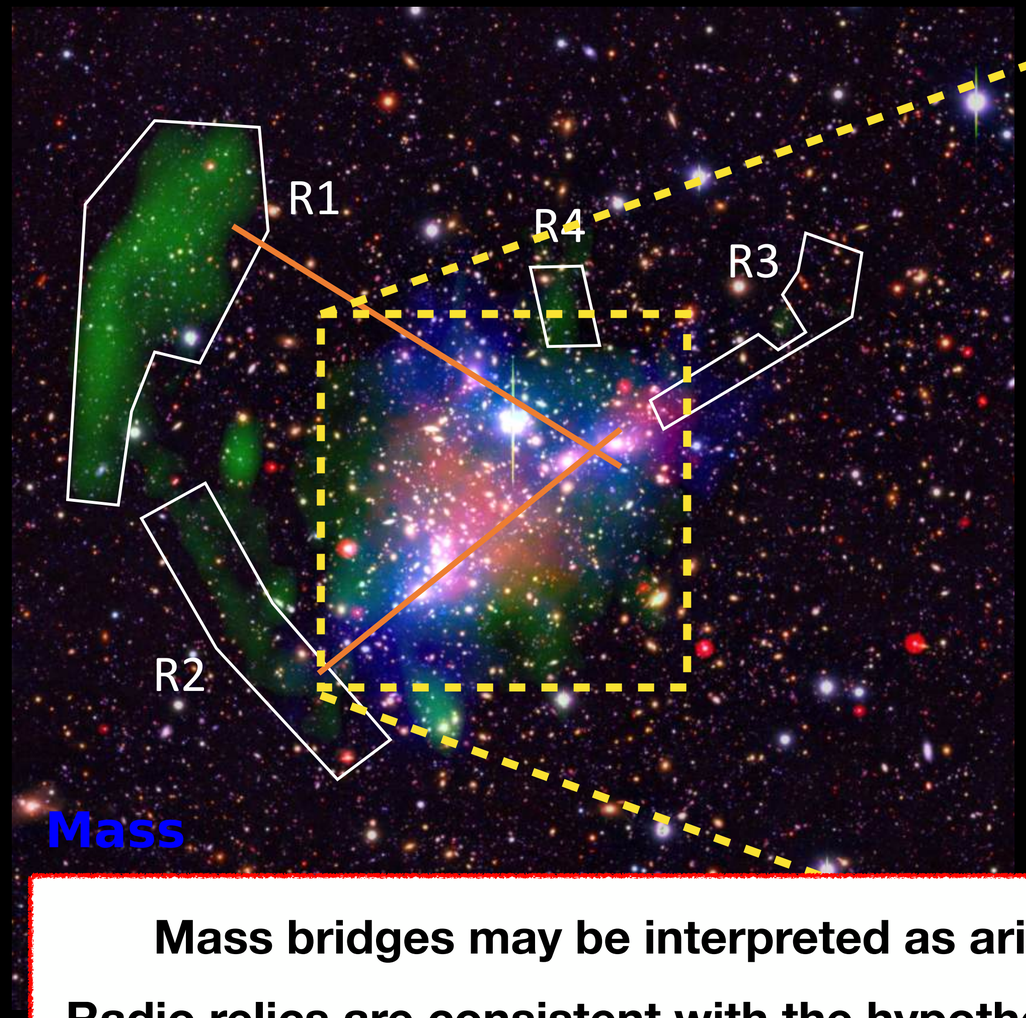


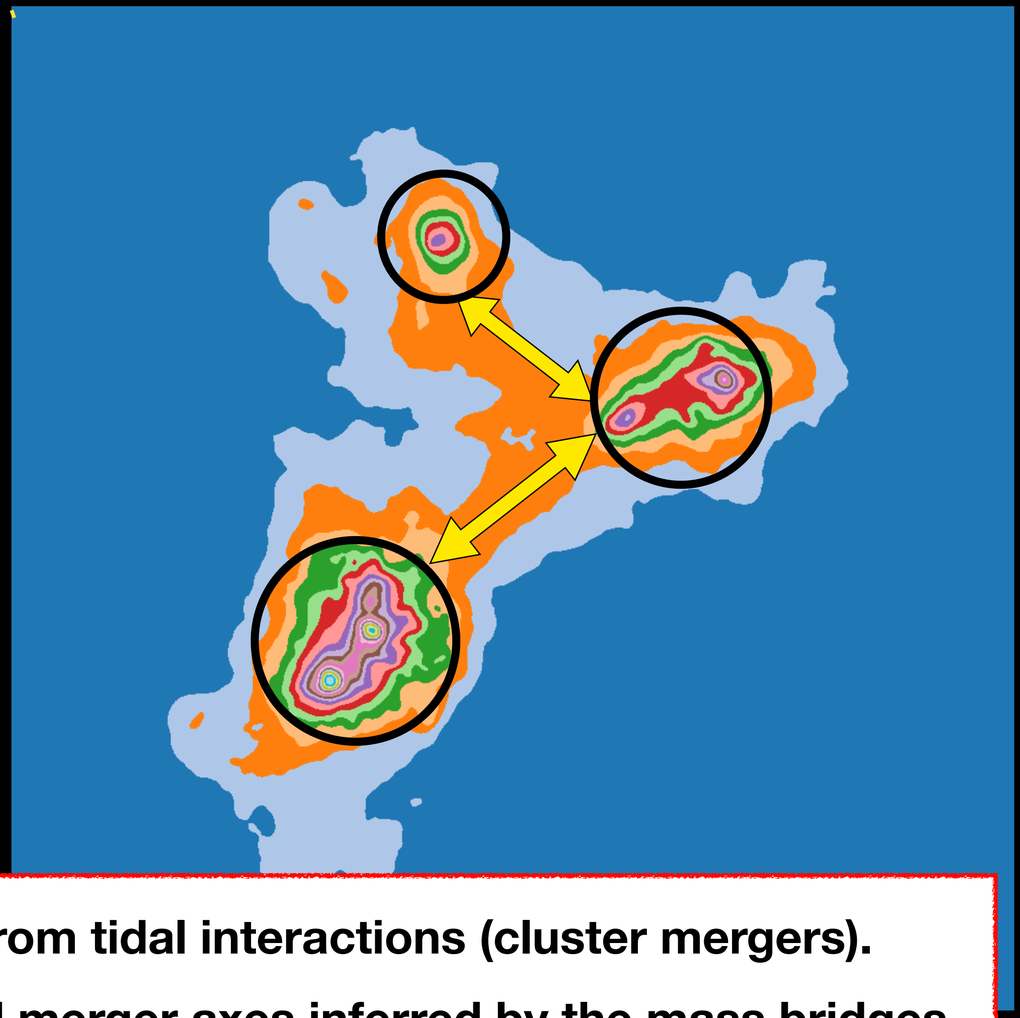


Cha et al. (2024); arXiv:2308.14805

Mass Map from MARS

Mass Bridges





Mass bridges may be interpreted as arising from tidal interactions (cluster mergers).

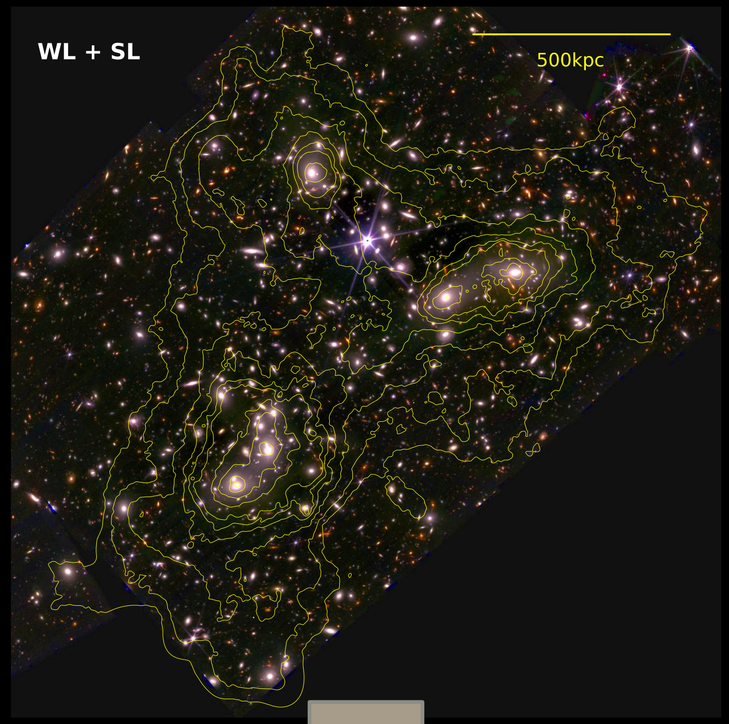
Radio relics are consistent with the hypothesized merger axes inferred by the mass bridges.

Cha et al. (2024); arXiv:2308.14805

Summary

Combining WL and SL

Model-independent Mass Reconstruction using MARS



Large Datasets from the Deep JWST Observations

Multi-wavelength Observations

Mass bridges (hypothesized merger axes)

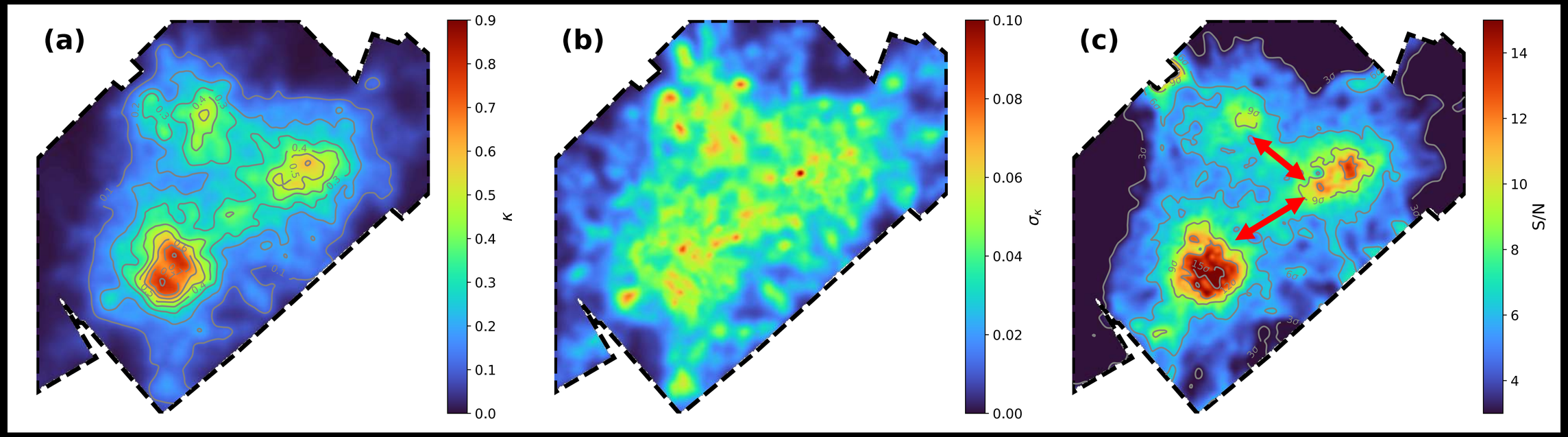
Probing Dark Matter Distributions

Evolution History of the Galaxy Clusters

arXiv:2308.14805
Published in ApJ

Thank you!

Significant level of the mass bridge



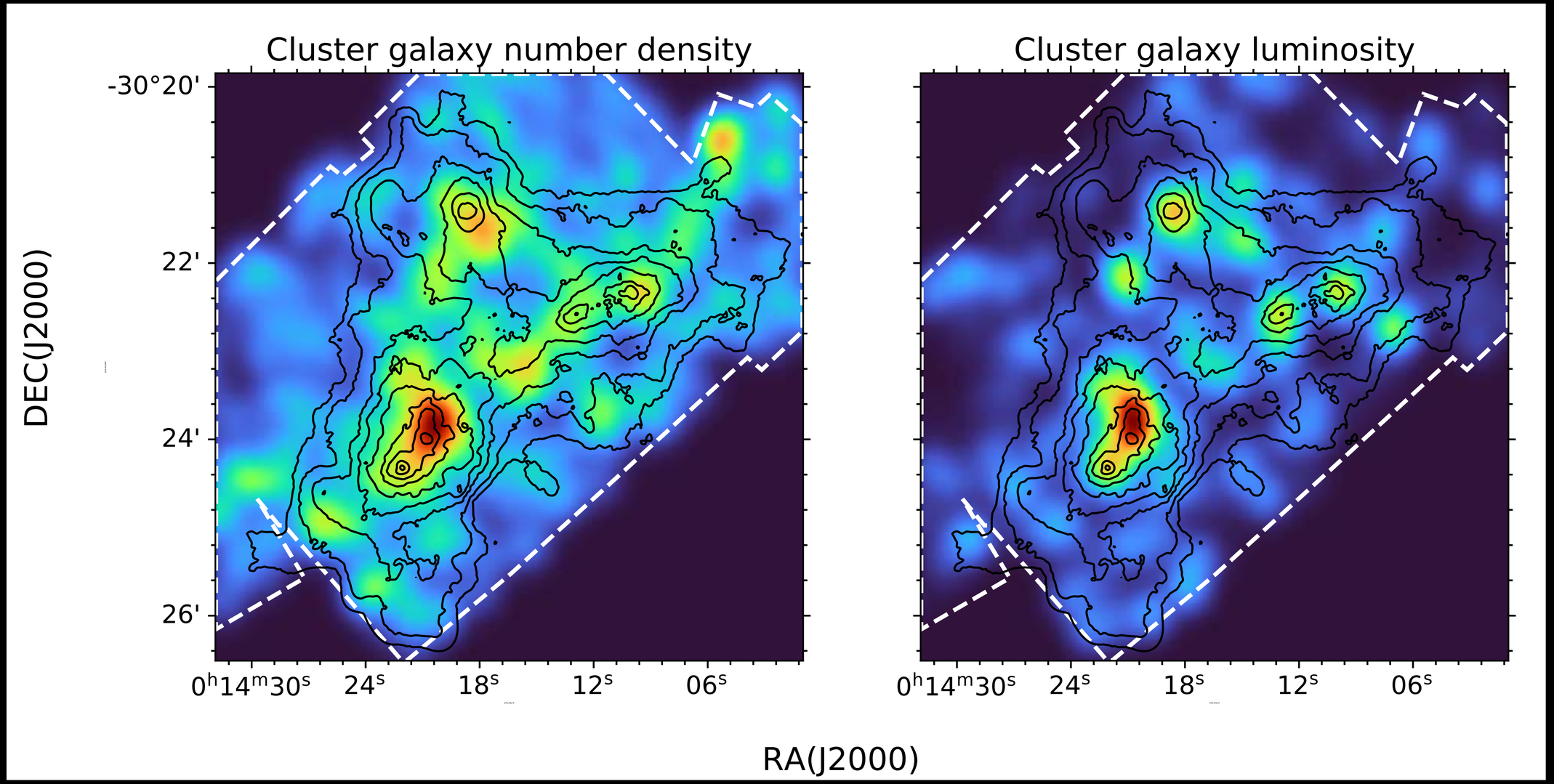
WL mass contours

WL mass uncertainty

WL S/N map

Cha et al. (2024); arXiv:2308.14805

Comparison to cluster member galaxies



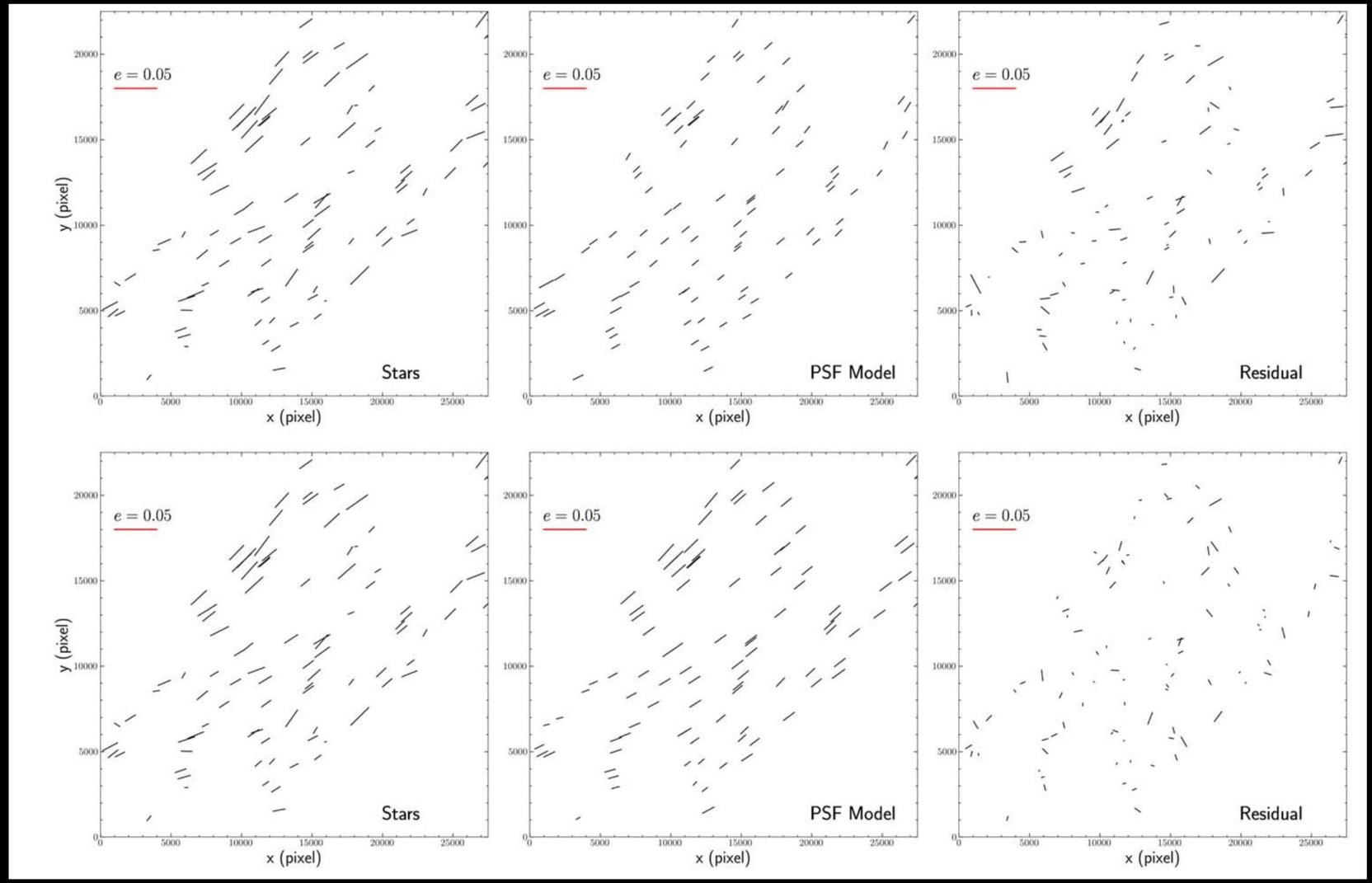
Cha et al. (2024); arXiv:2308.14805

PSF Modeling

WebbPSF vs. Empirical Modeling

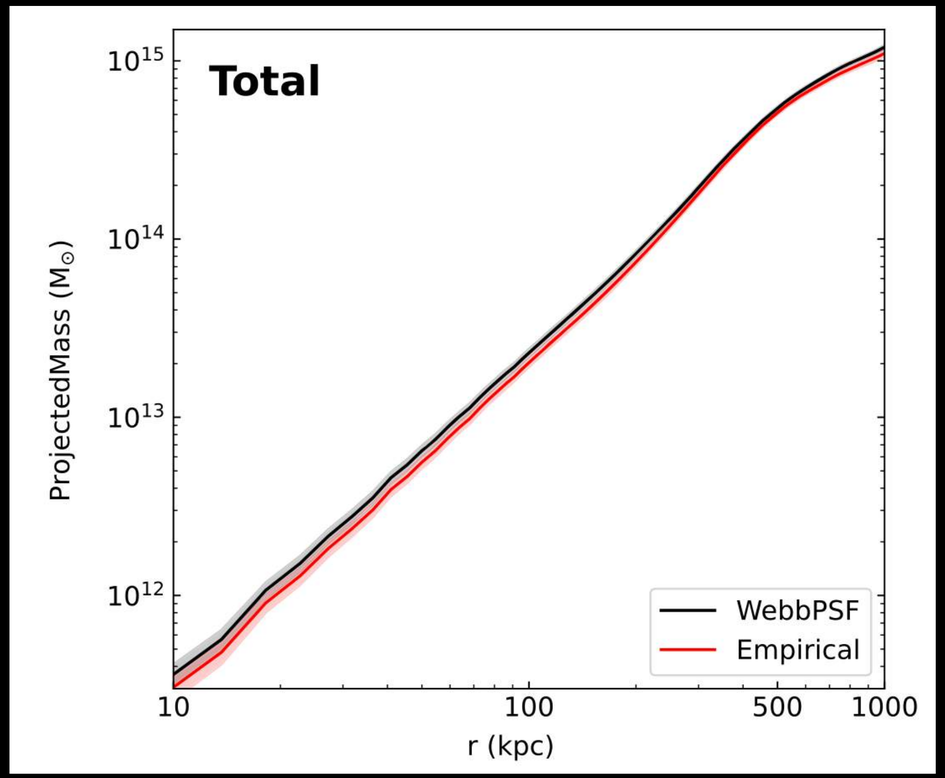
WebbPSF

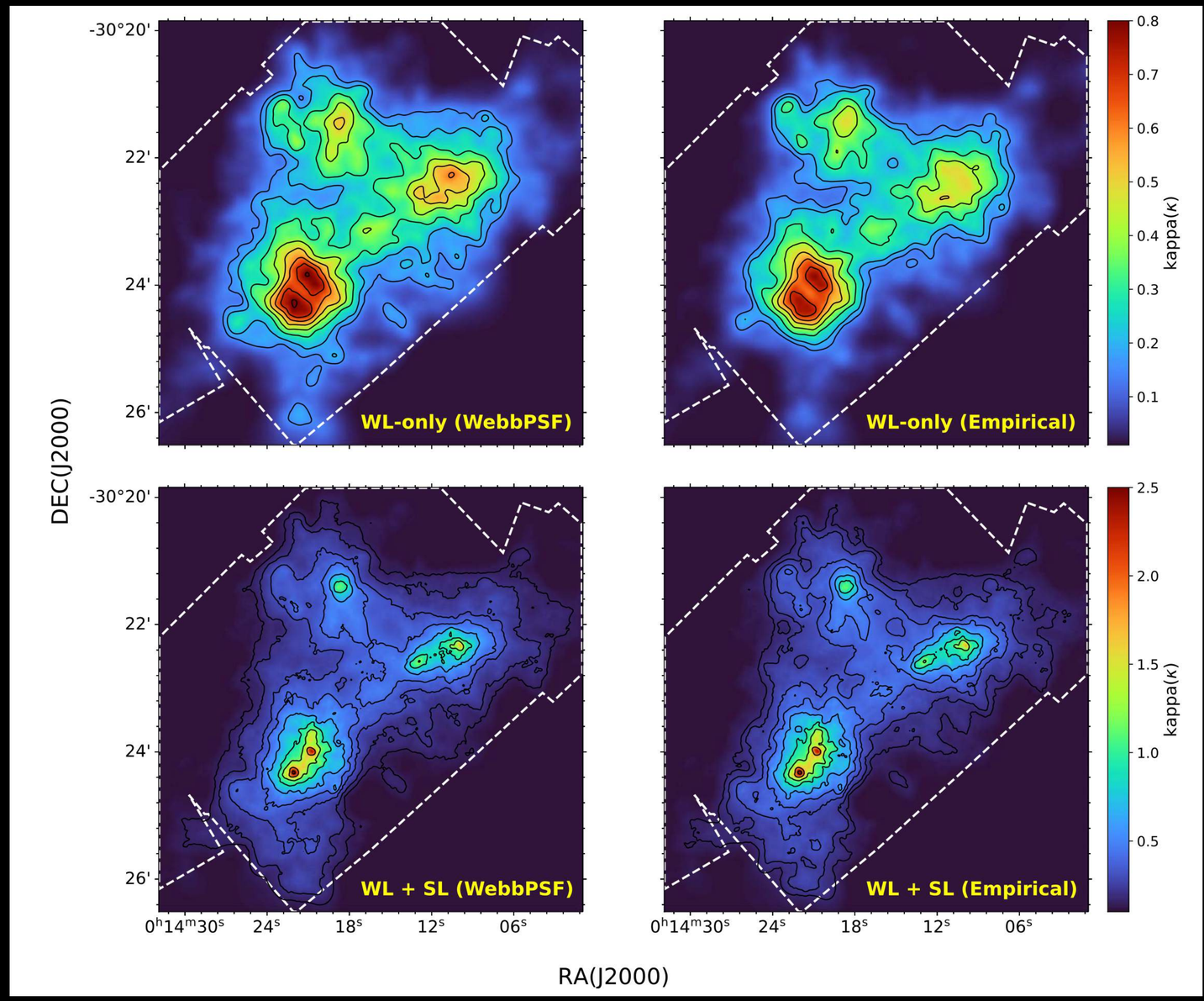
Empirical Modeling



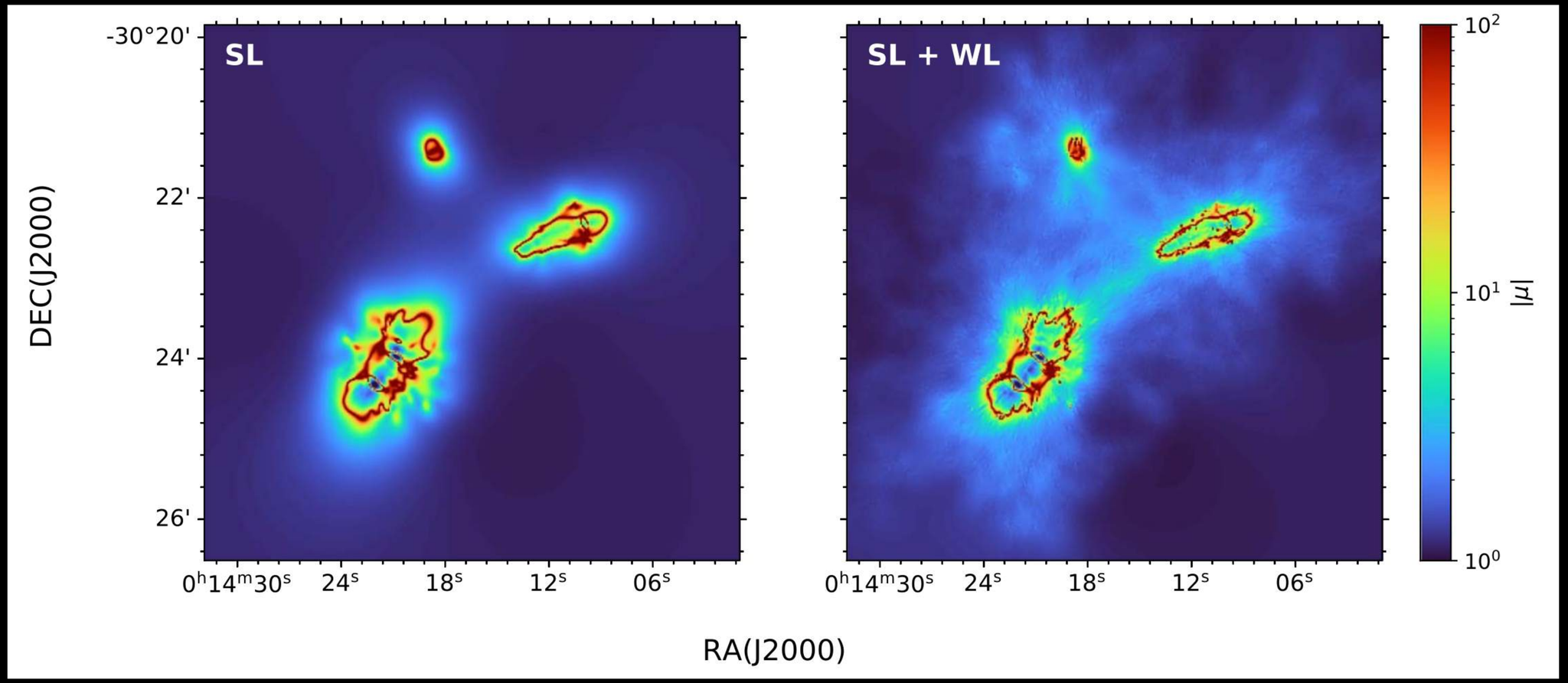
PSF Modeling

WebbPSF vs. Empirical Modeling

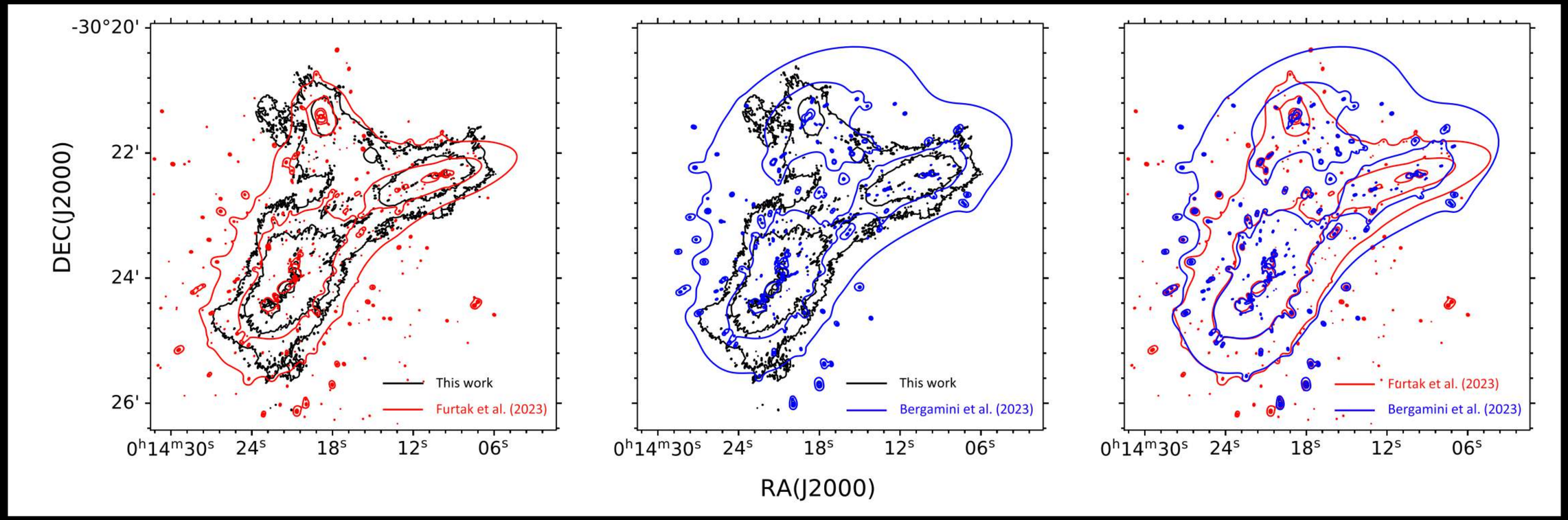




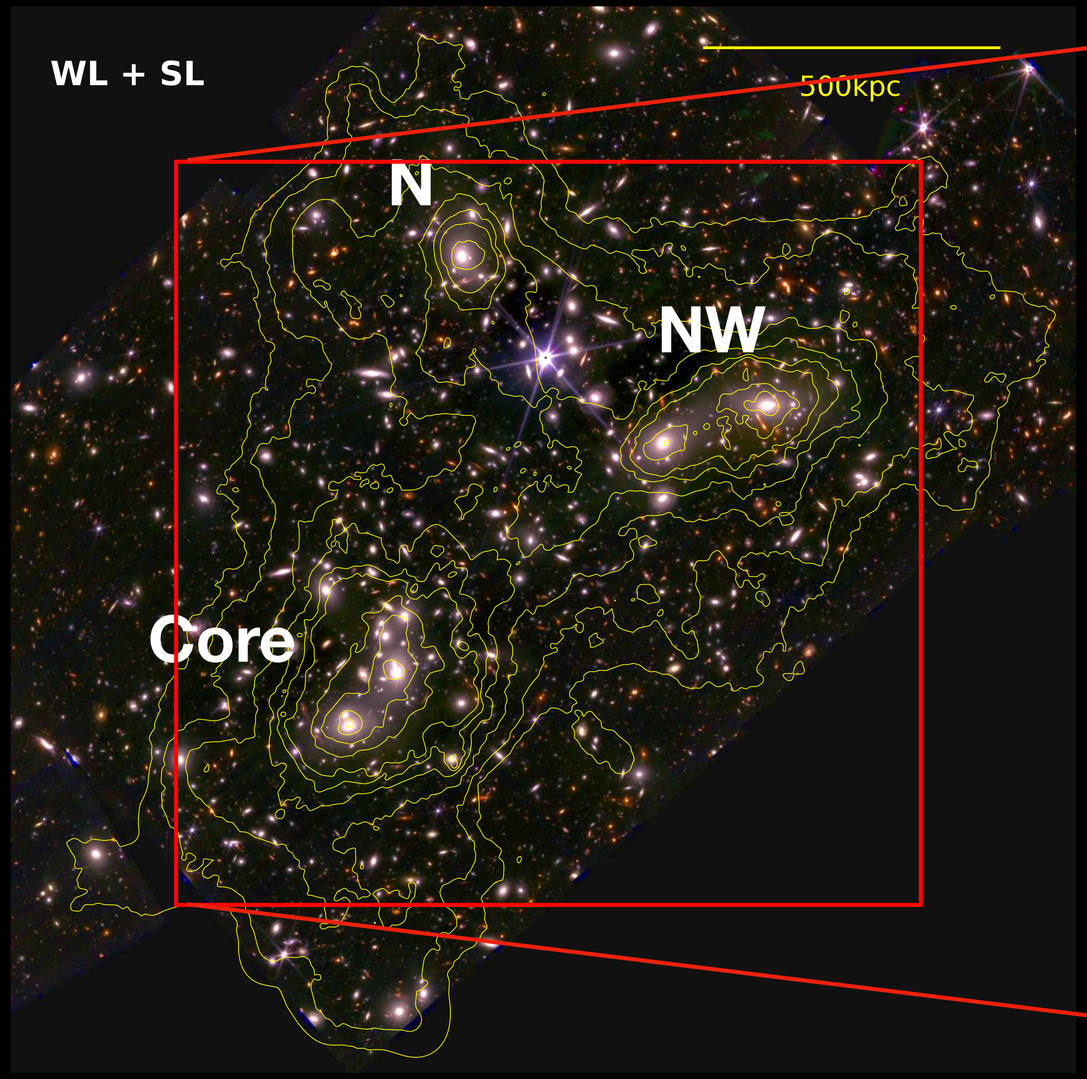
Magnification

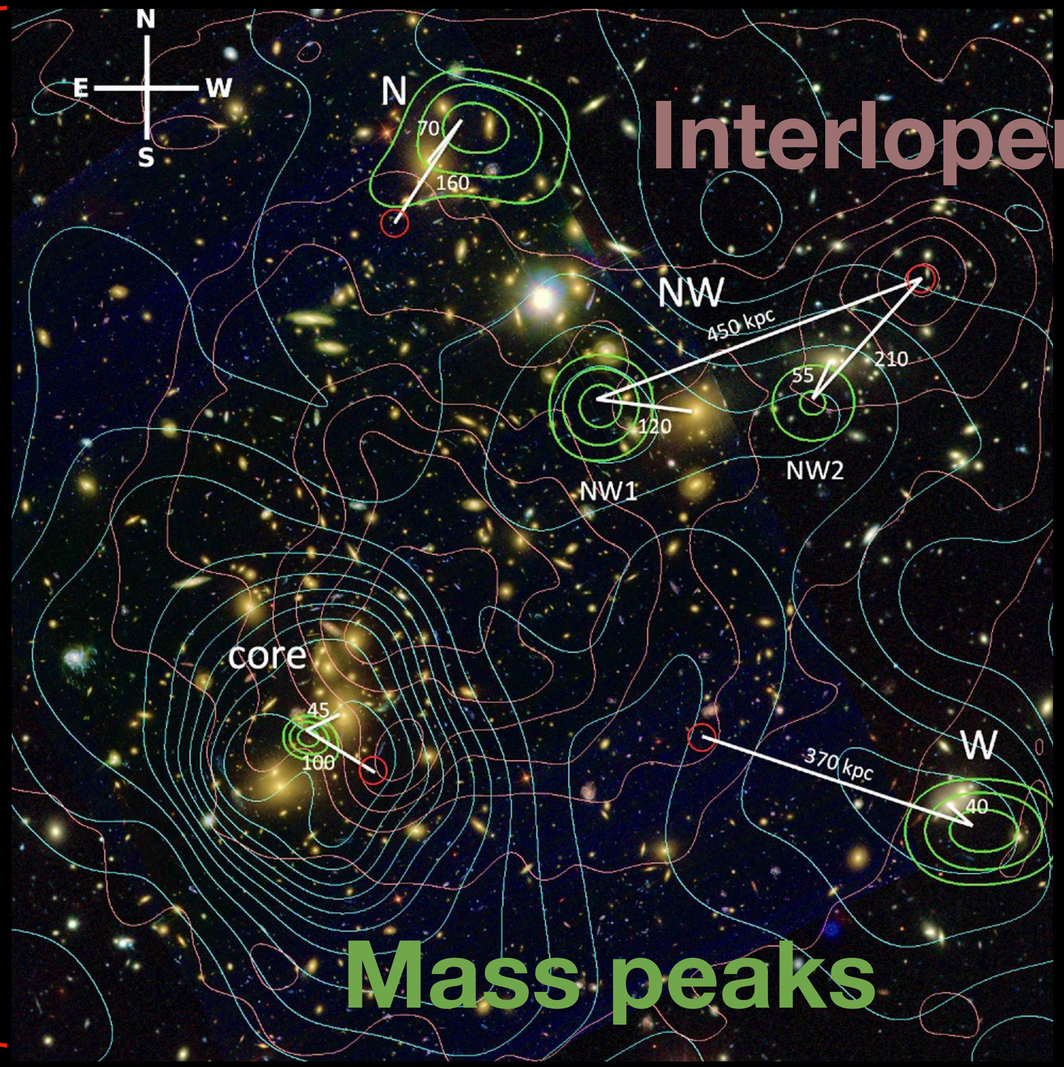


Magnification



No More Offsets, No More Dark Clump





Cha et al. (2024); arXiv:2308.14805

Merten et al. (2011); arXiv:1103.2772

Robustness test of SL

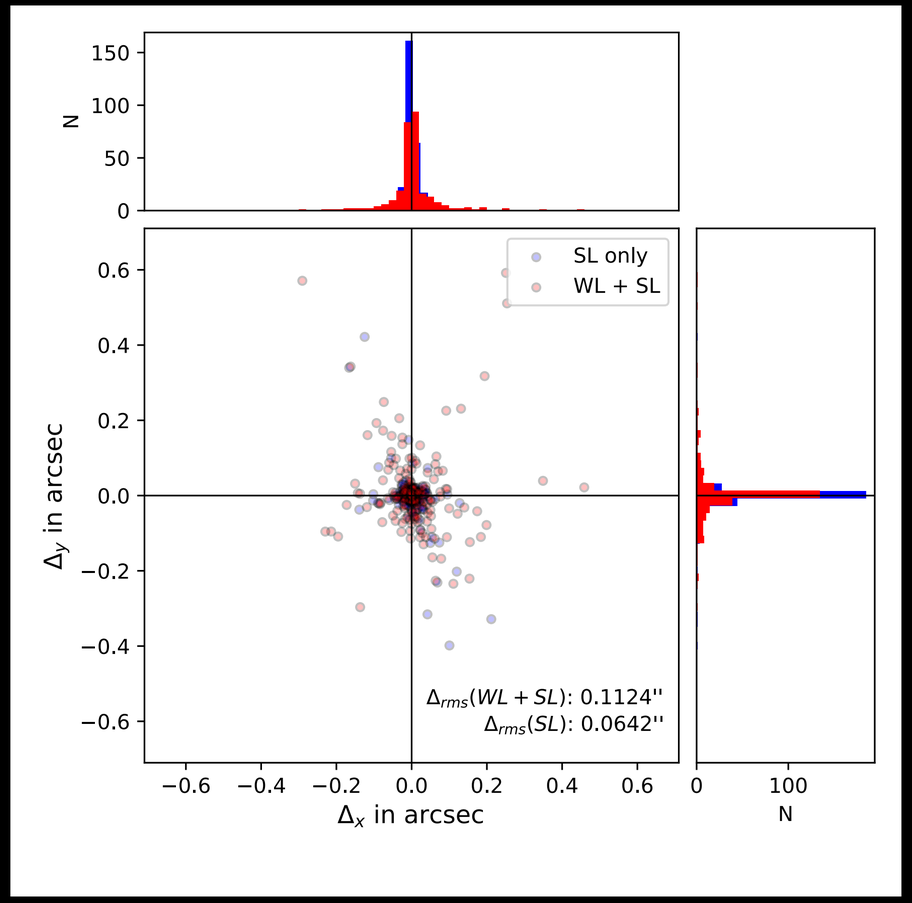
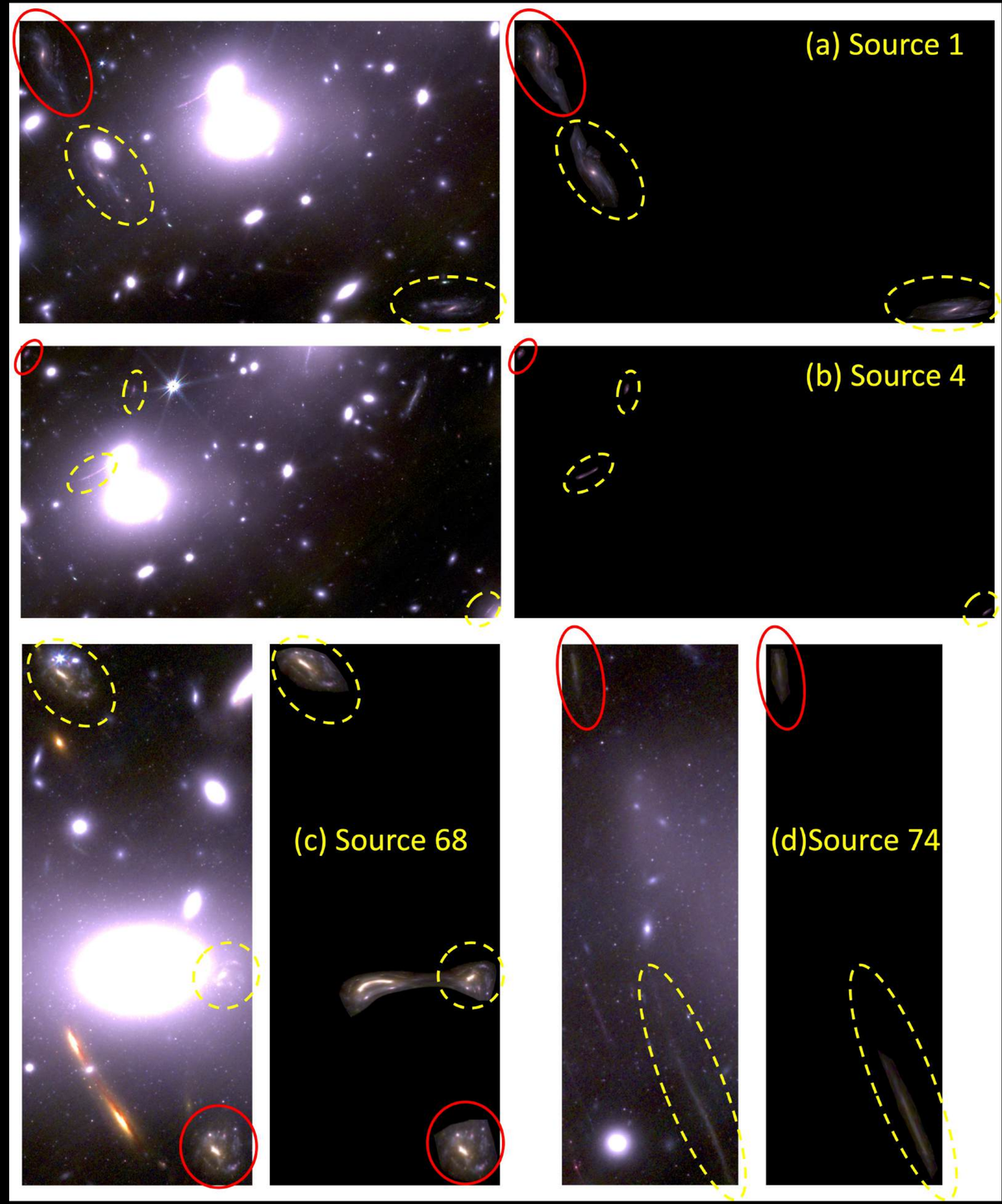
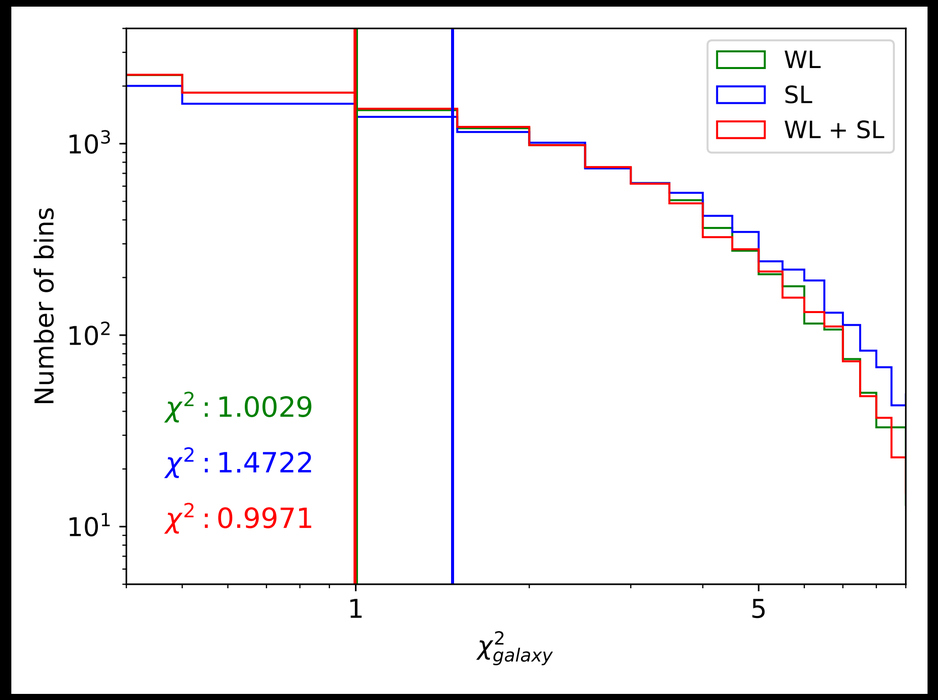


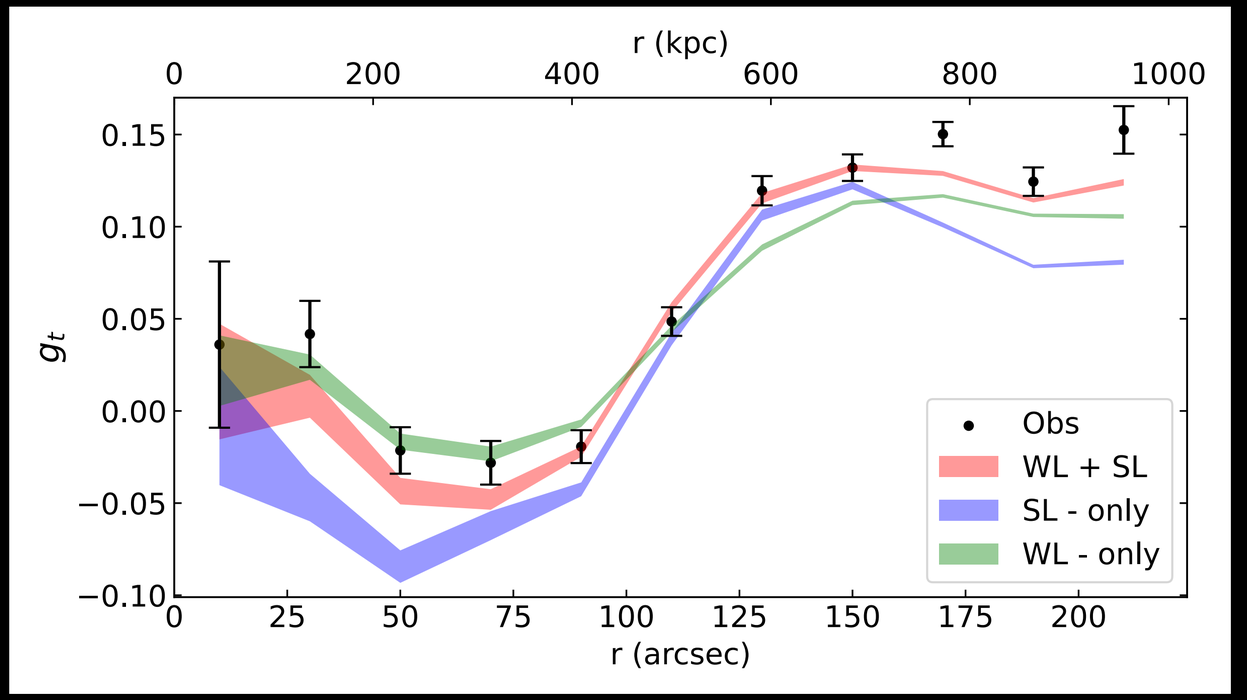
Image plane scatter between
observed and predicted multiple images



Cha et al. (2024); arXiv:2308.14805

Robustness test of WL





$$\chi^2_{galaxy} = \frac{(g_{i,j} - \epsilon_{i,j})^2}{\sigma_s^2(g) + \sigma_{m,i}^2}$$

$$g_+ = -g_1 cos2\phi - g_2 sin2\phi$$

$$[\bar{\kappa}(<r) - \kappa(r)]/[1 - \kappa(r)]$$

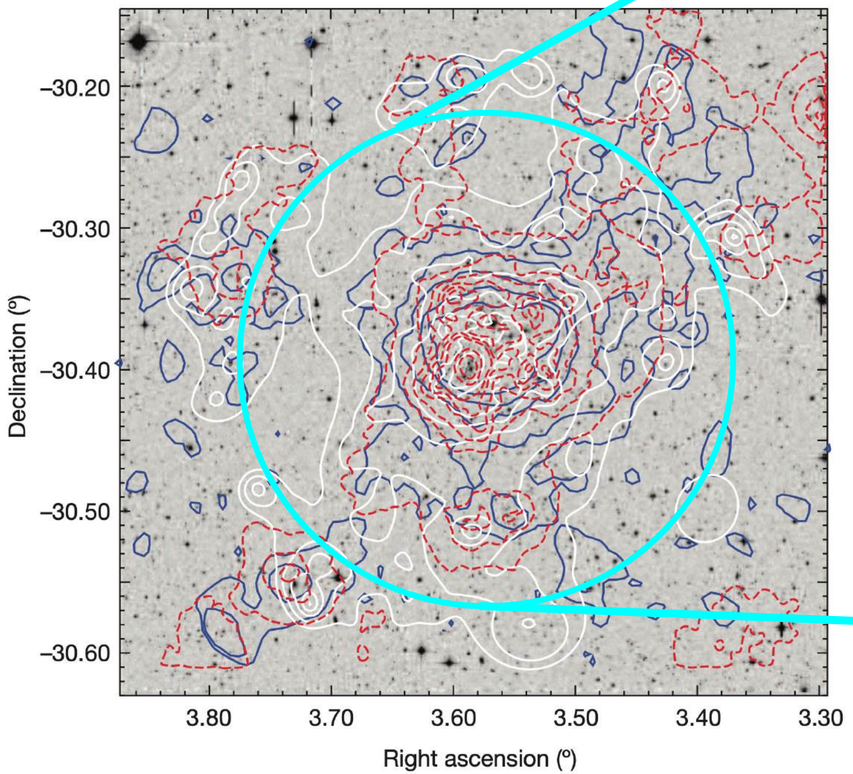
Cha et al. (2024); arXiv:2308.14805

Wide-field WL+SL

- Eckert et al. 2015

- Red: optical
- Blue: X-ray
- White: WL+SL

- WL only mass map (JWST + SC)



MAximum-entropy ReconStruction (MARS)

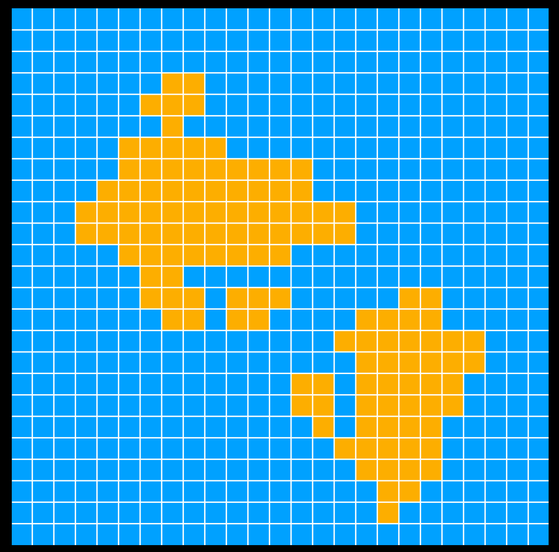
Free-form vs. Parametric Method

- **Parametric method**



- Small number of free parameters
- Lack of flexibility

- **Free-form method**

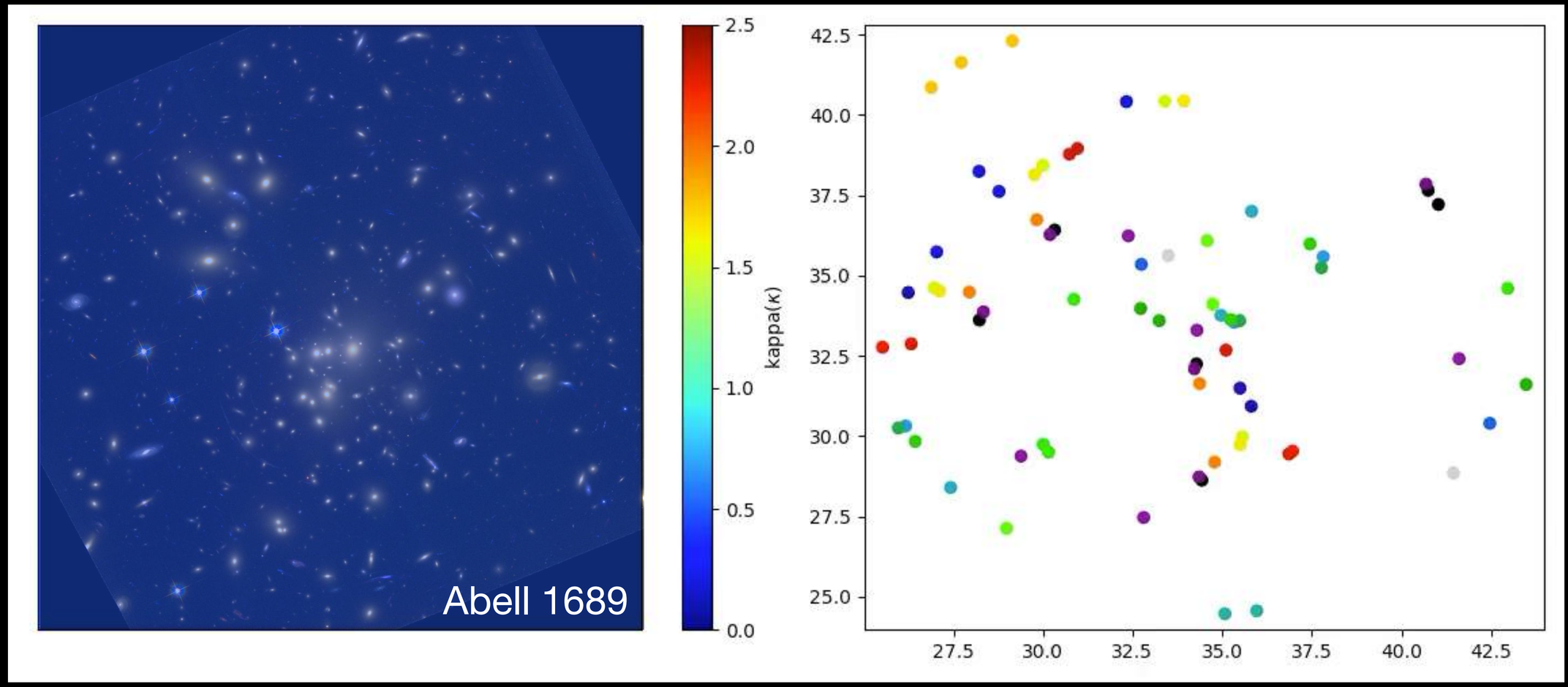


- Large number of free parameters
- Flexibile mass maps

Cha & Jee (2022); arXiv:2202.10489

MARS Mass Reconstruction

Abell 1689 Example



- Mass map

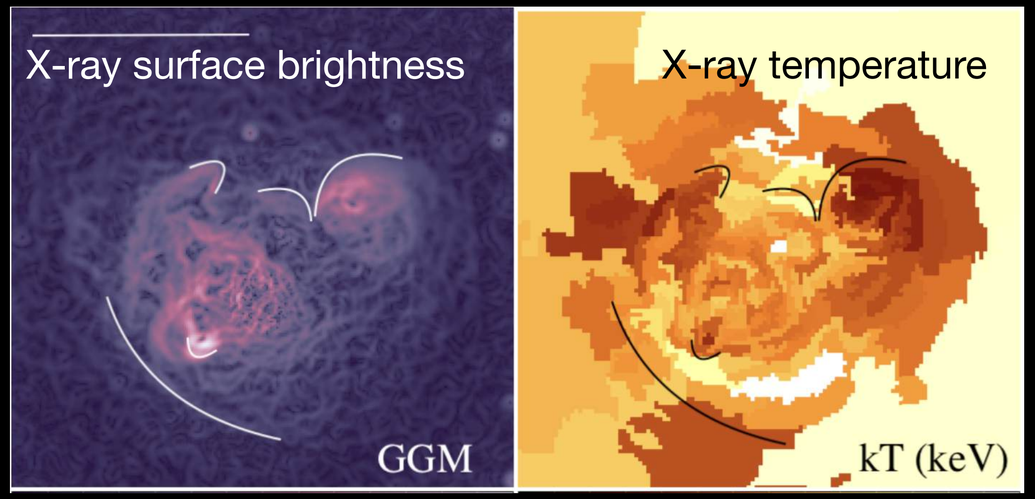
- Locations of multiple images in their source redshifts
- Same color: images from the same source

Cha & Jee (2022); arXiv:2202.10489

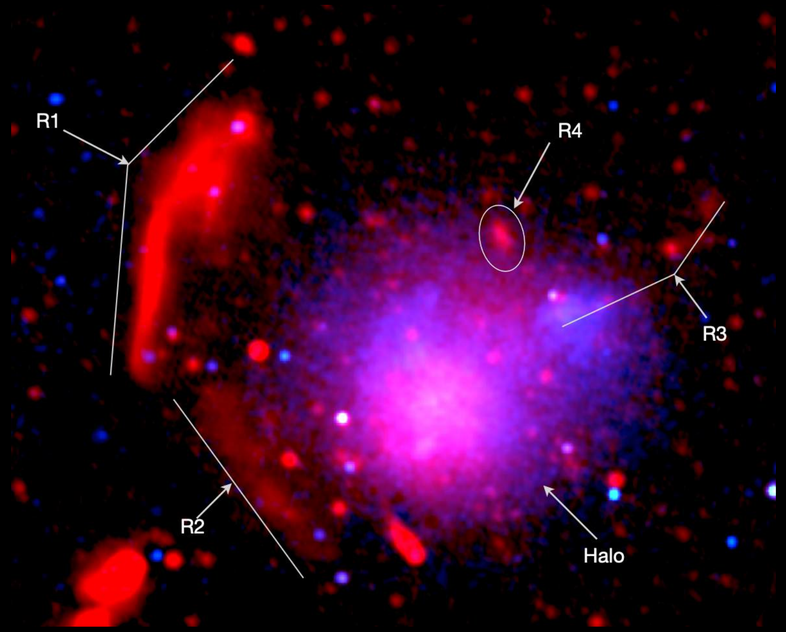
Further Analysis

DM + X-ray + Radio



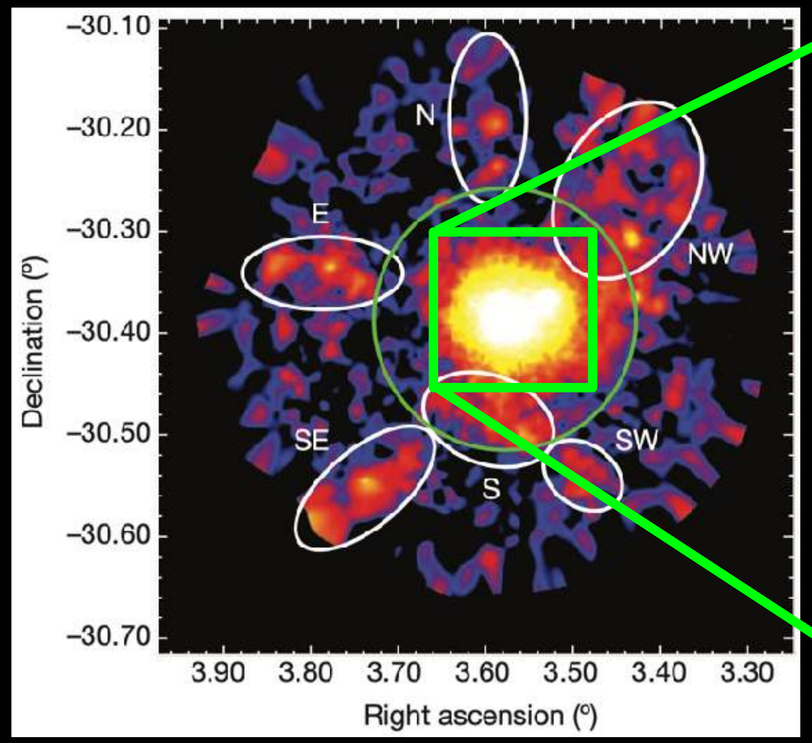


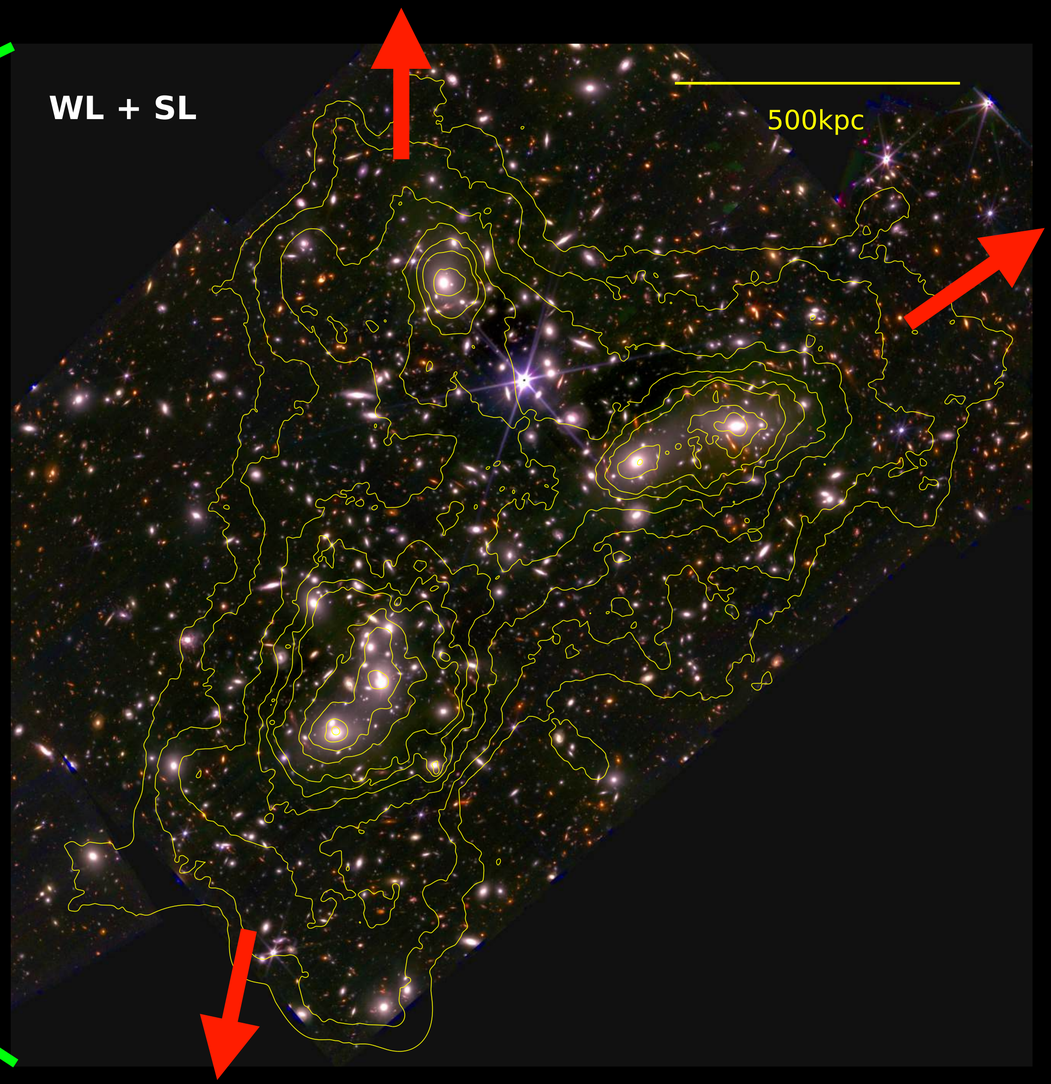
Chadayammuri et al. (2024); arXiv:2407.03142



Rajpurohit et al. (2021); arXiv:2104.05690

Filamentary structure around A2744





Eckert et al. (2015); arXiv:1512.00454

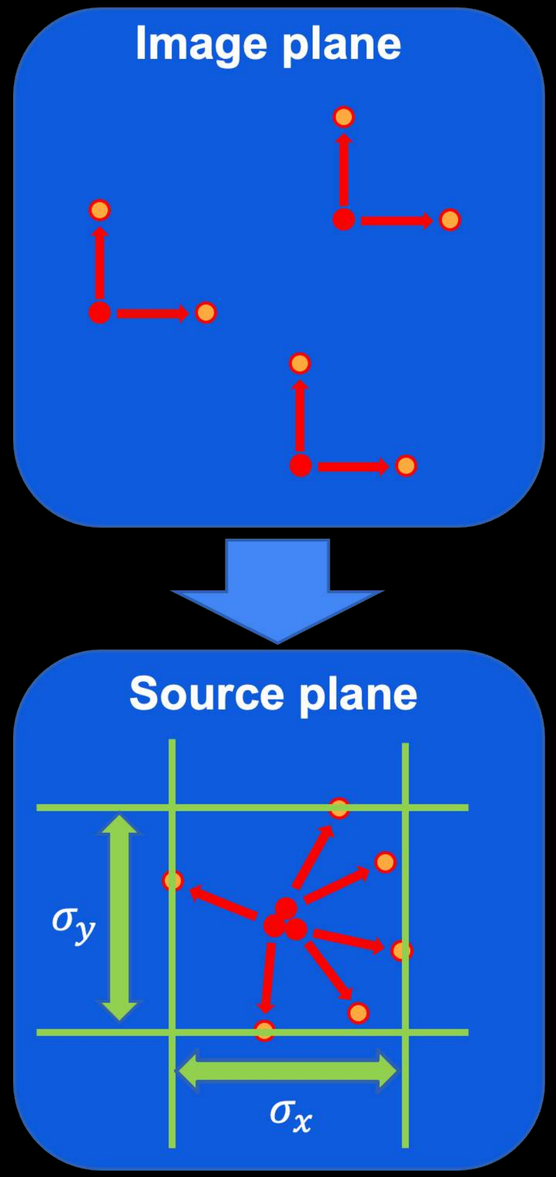
Cha et al. (2024); arXiv:2308.14805

Employing virtual knots

$$f = m\chi^2_{SL} + w\chi^2_{WL} + rR$$

$$\chi^2_{SL} = \Sigma\frac{(\theta - \alpha(\theta, z) - \beta)^2}{\sigma^2} \qquad \chi^2_{WL} = \sum\frac{(g_{obs} - g_{pre})^2}{\sigma_s^2 + \sigma_m^2} \qquad R = \Sigma(p - \kappa + \kappa\ln\frac{\kappa}{\mathrm{p}})$$

$$\sigma^2 = \sigma_x^2 + \sigma_y^2$$

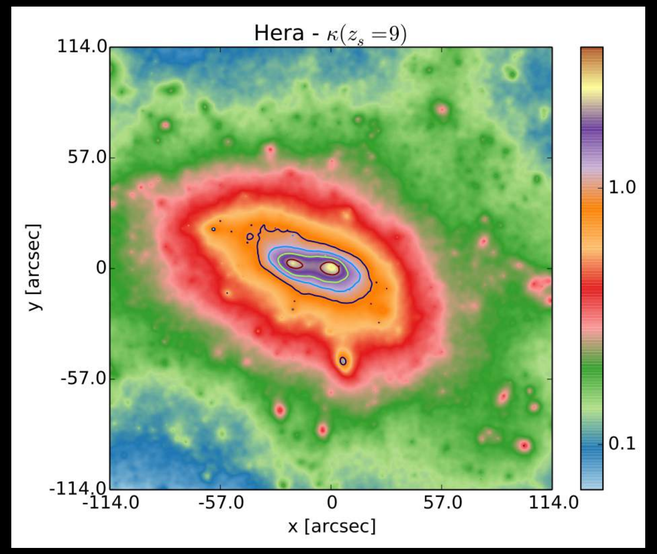


- We consider magnification information indirectly by employing virtual knots.
- This approach prevent an over-prediction of magnification (overfitting).

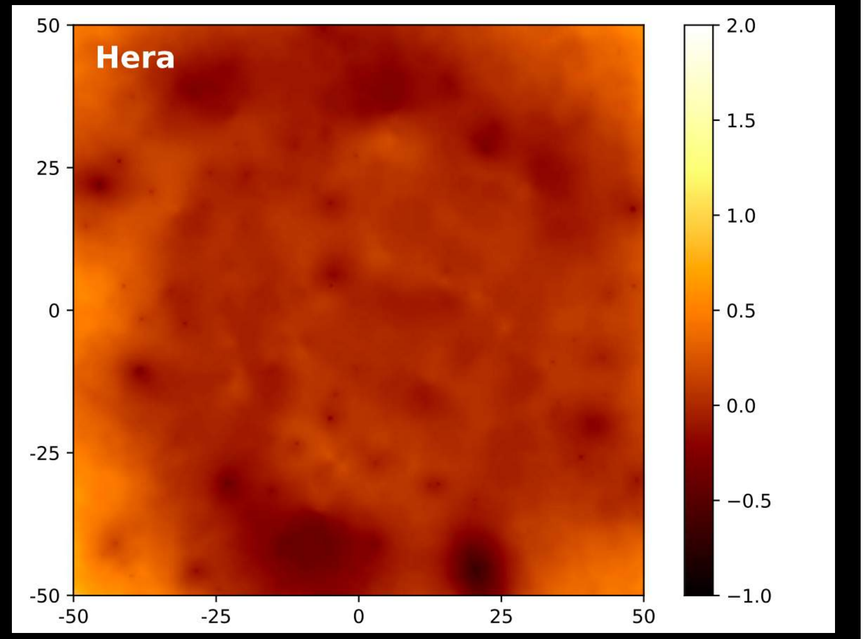
Cha & Jee (2022); arXiv:2202.10489

Performance test using simulated clusters

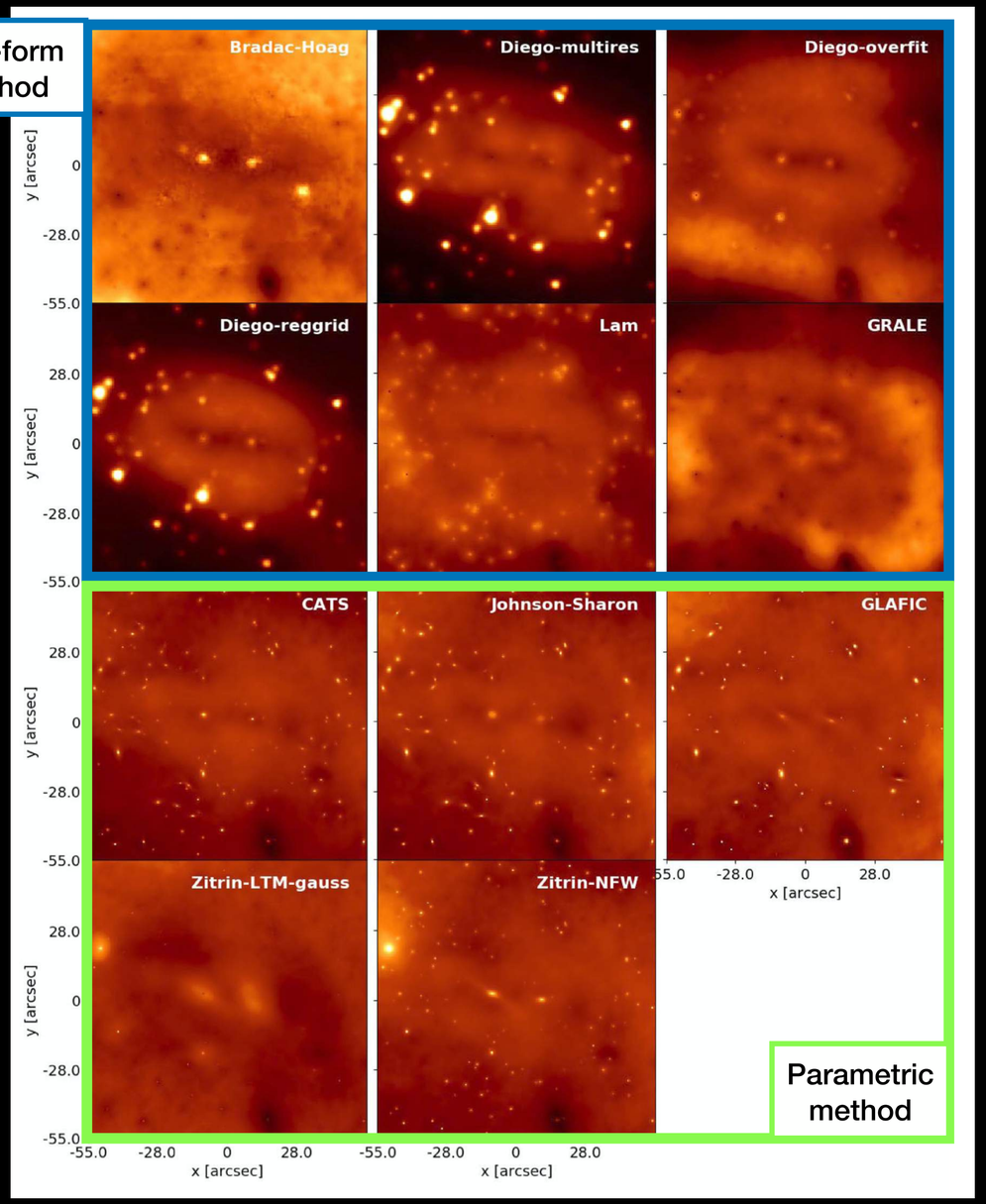
κ residual: $(\kappa - \kappa_{truth})/\kappa_{truth}$



- Truth κ map

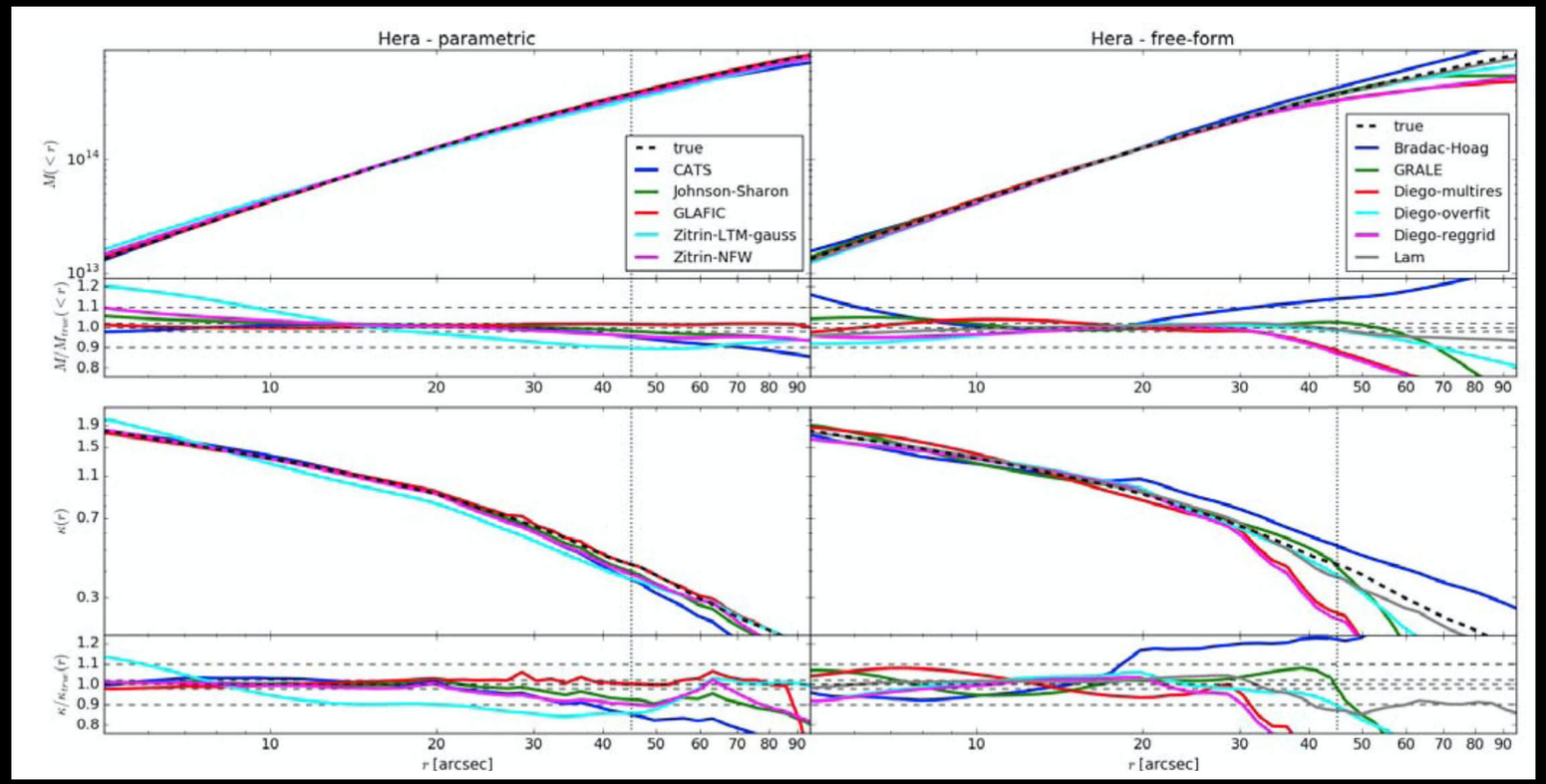


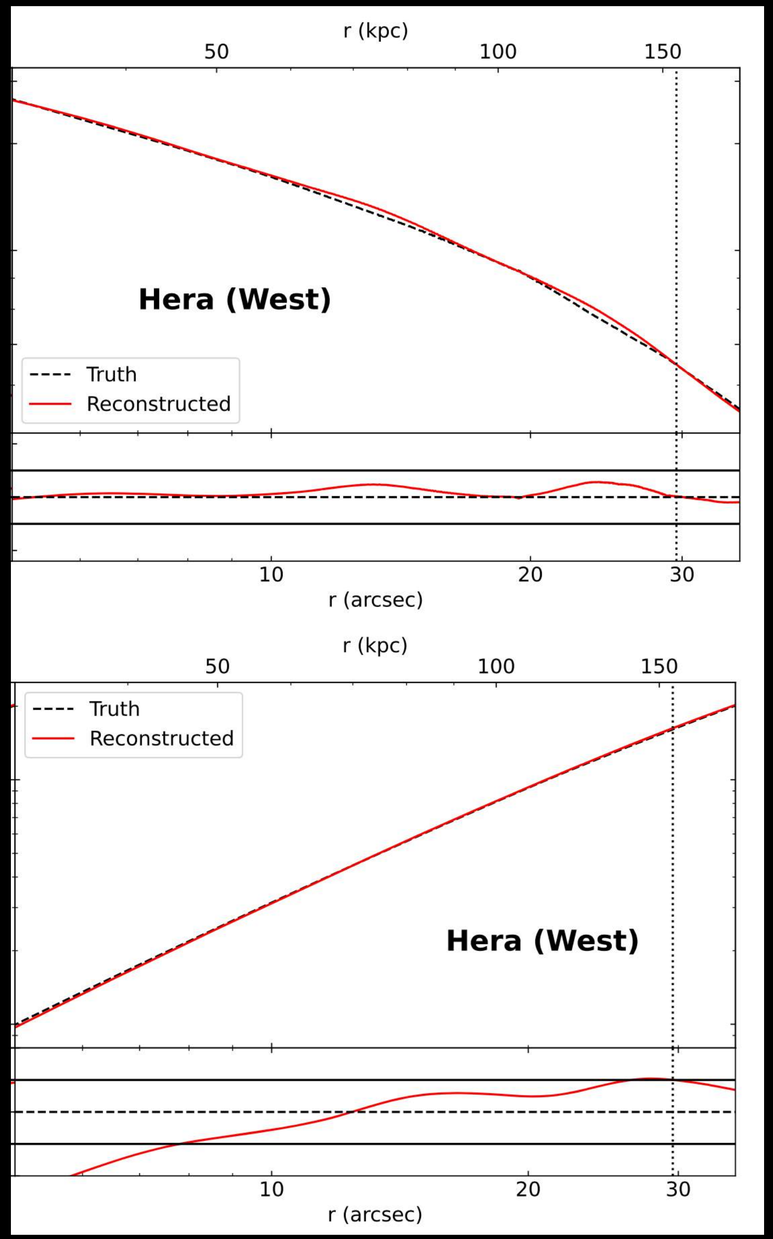
- κ residual from the MARS algorithm



Meneghetti et al. (2017); arXiv:1606.04548
Cha & Jee (2022); arXiv:2202.10489

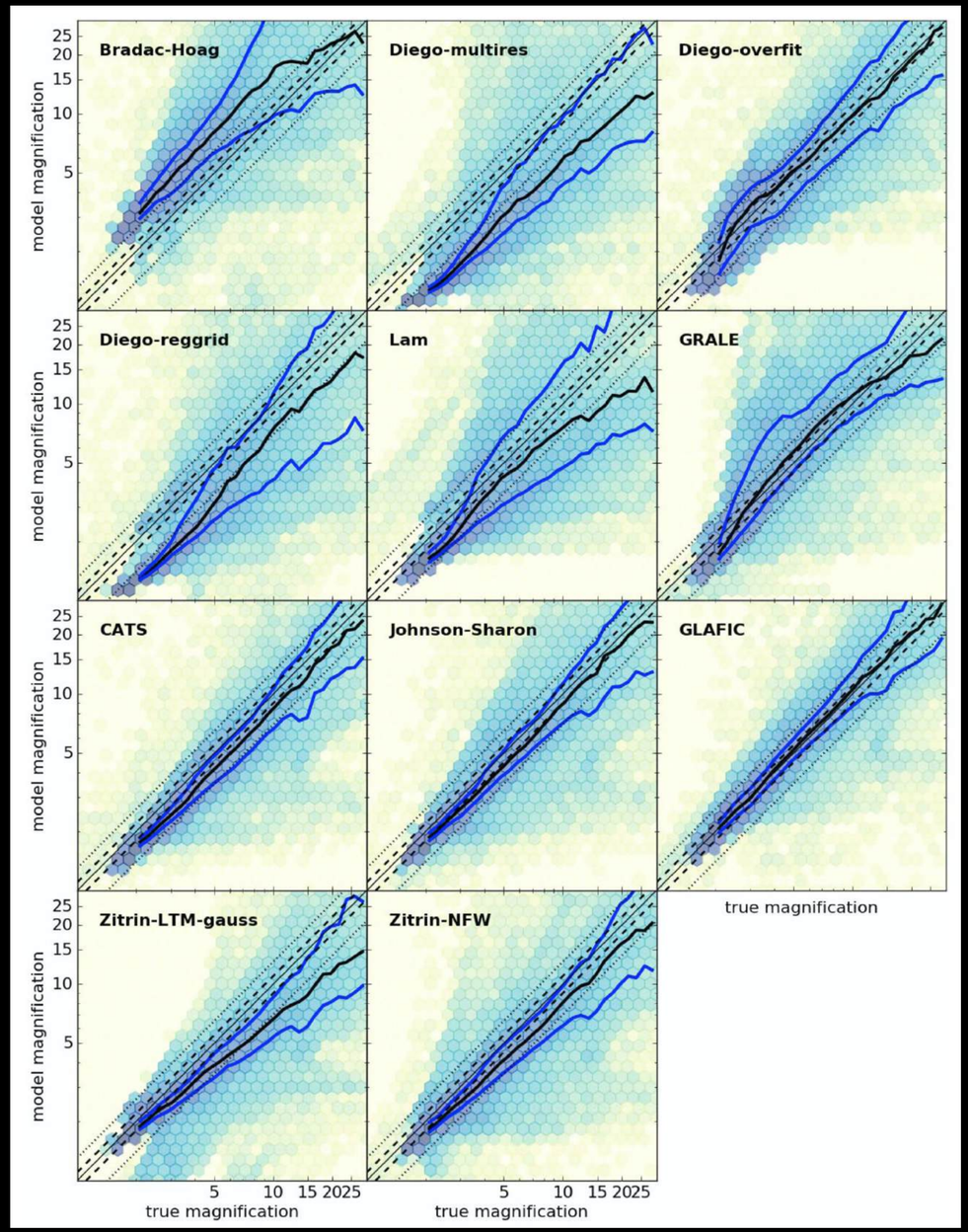
Performance test using simulated clusters

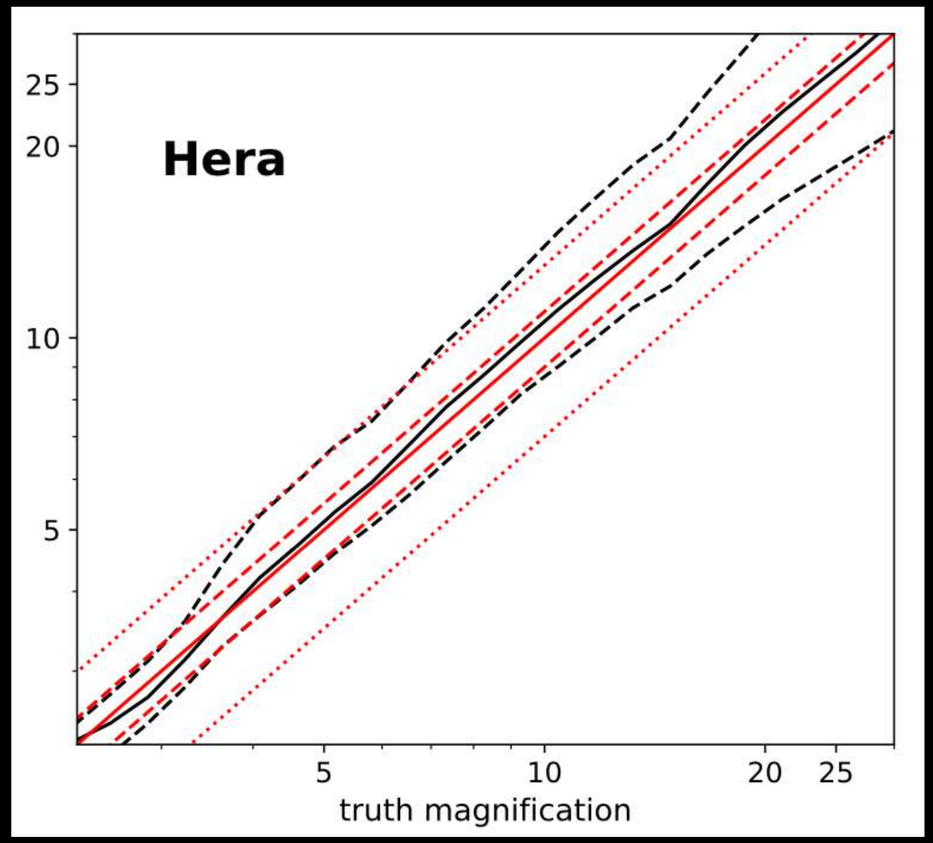




Meneghetti et al. (2017); arXiv:1606.04548
Cha & Jee (2022); arXiv:2202.10489

Performance test using simulated clusters



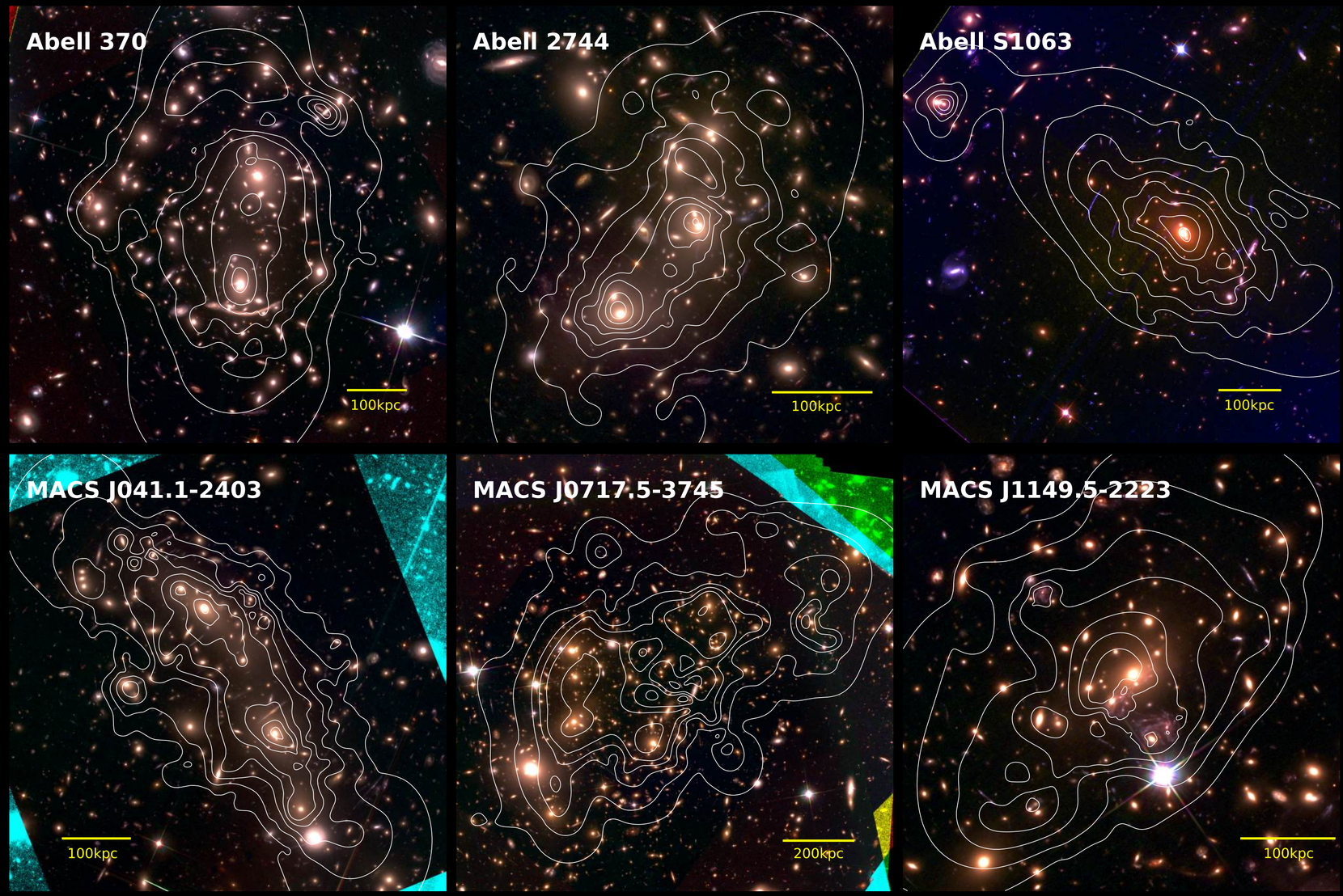


- Black solid line: median of magnifications
- Black dashed lines: 25th & 75th percentiles
- Red solid line: perfect correlation
- Red dashed lines: ±10% differences
- Red dotted lines: ±30% differences

Meneghetti et al. (2017); arXiv:1606.04548

Cha & Jee (2022); arXiv:2202.10489

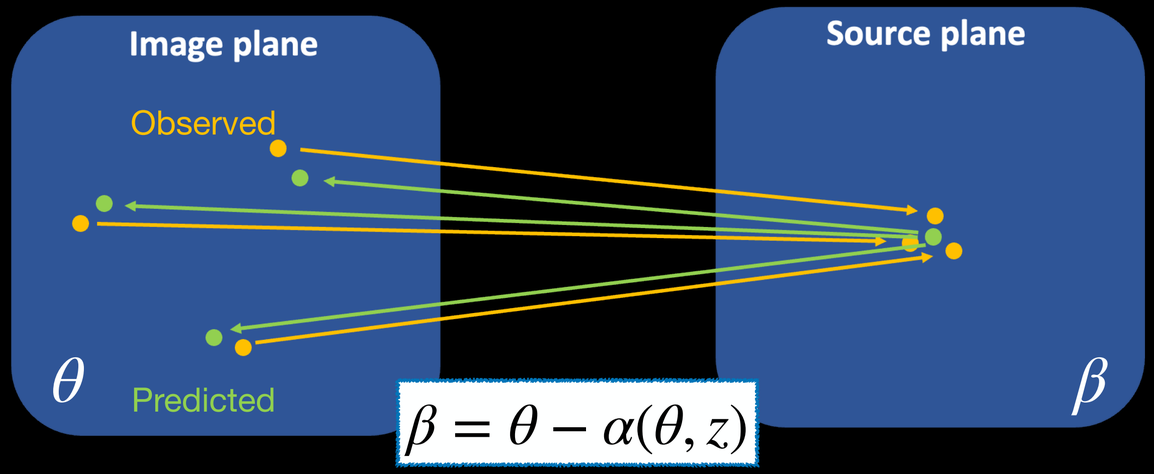
Mass maps of the HFF clusters from MARS



Cha & Jee (2023); arXiv:2301.08765

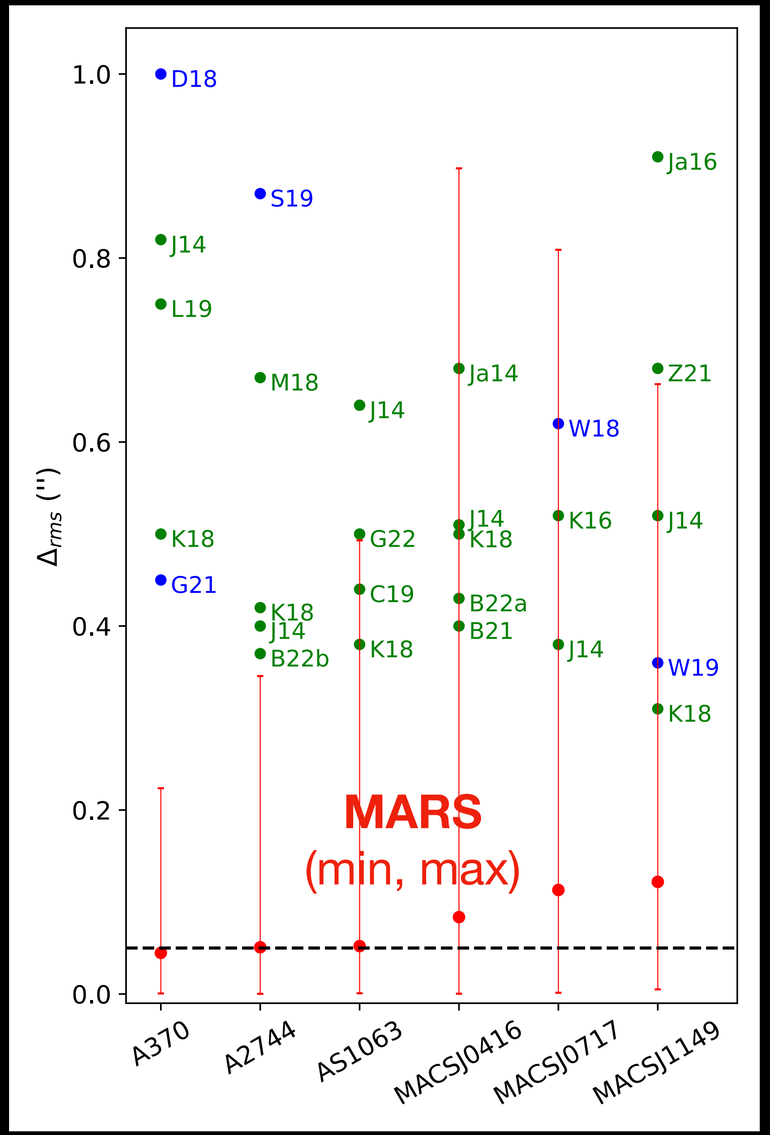
Application to real galaxy clusters

Accuracy comparison



- RMS between observed and predicted image locations from MARS is lower than other modeling algorithms.

- MARS is a powerful tool for SL modeling in the JWST era.

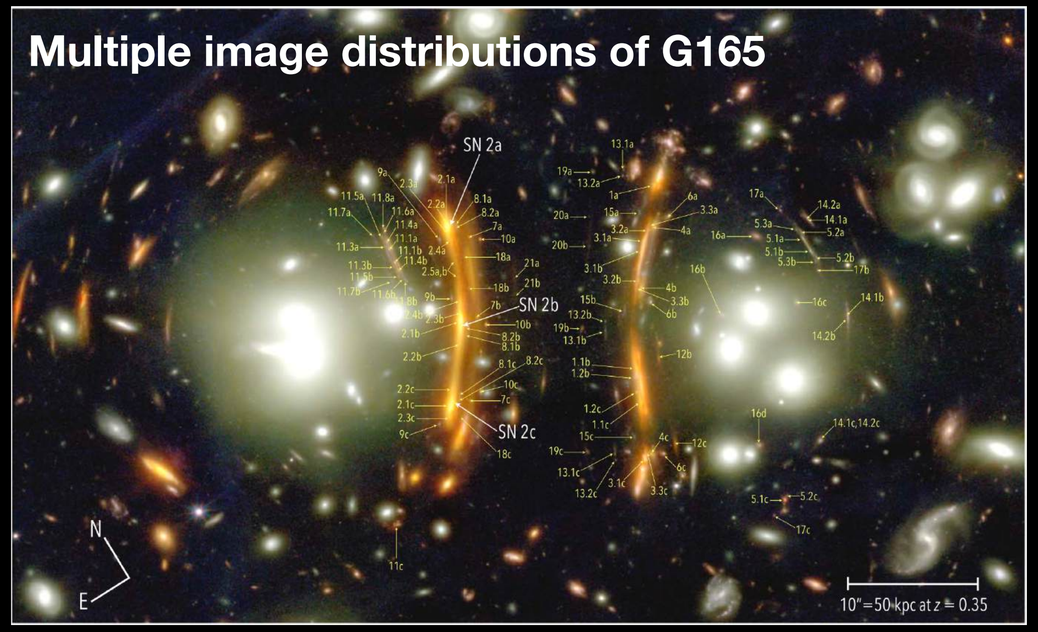


- Blue dots: results from the free-form methods
- Green dots: results from the parametric methods

Cha & Jee (2023); arXiv:2301.08765

Hubble constant inference

Blind analysis



- A total of 7 SL models are used for the Hubble constant inference.
- To avoid biases from humans, properties of lensed supernovae (like magnification, time-delay…) are **blinded**.
- We only utilized the location of multiple images for SL modeling.

Pierel et al. 2024; arXiv:2403.18954 (photometric analysis)

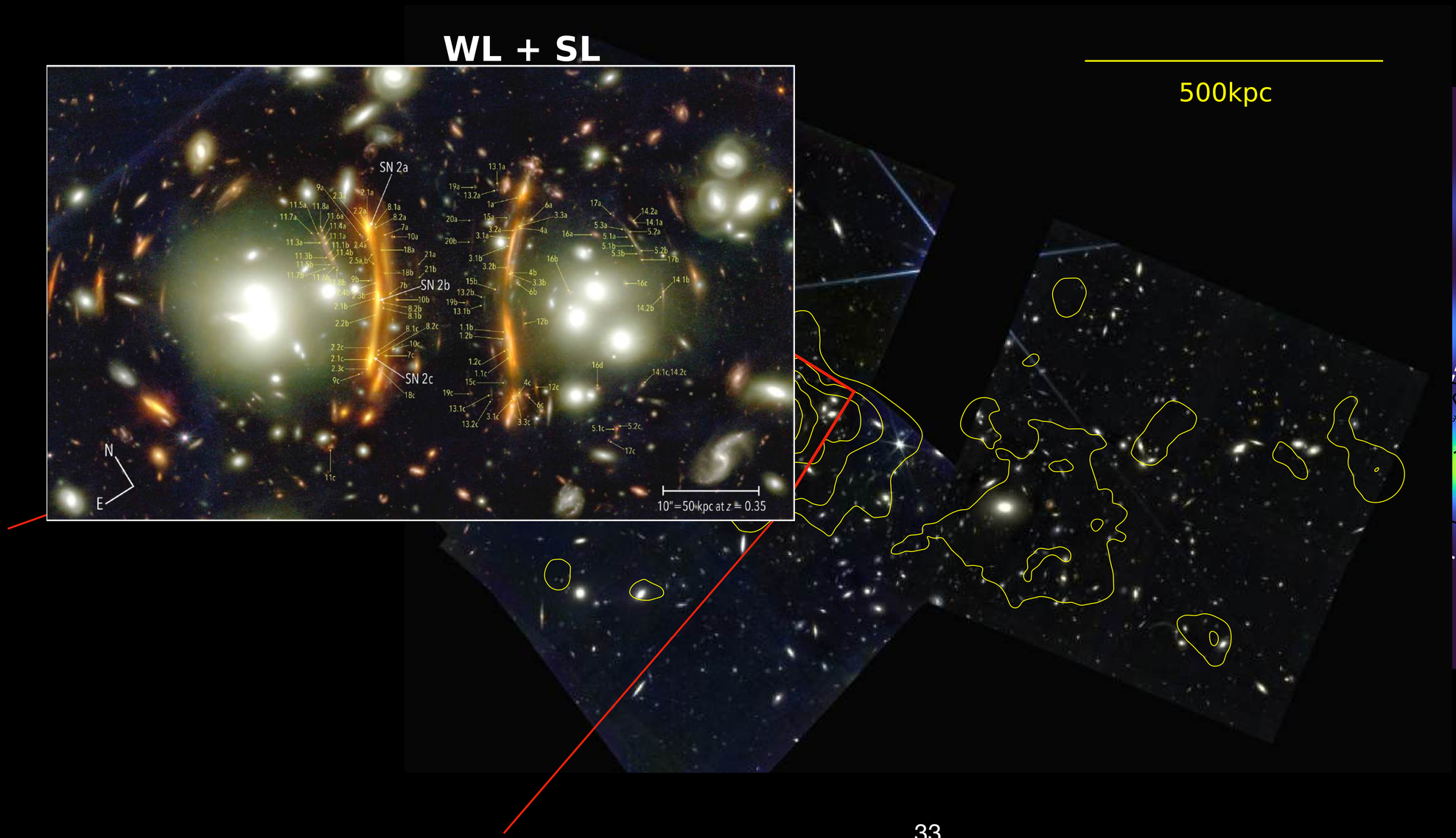
Chen et al. 2024; arXiv:2403.19029 (spectroscopic analysis)

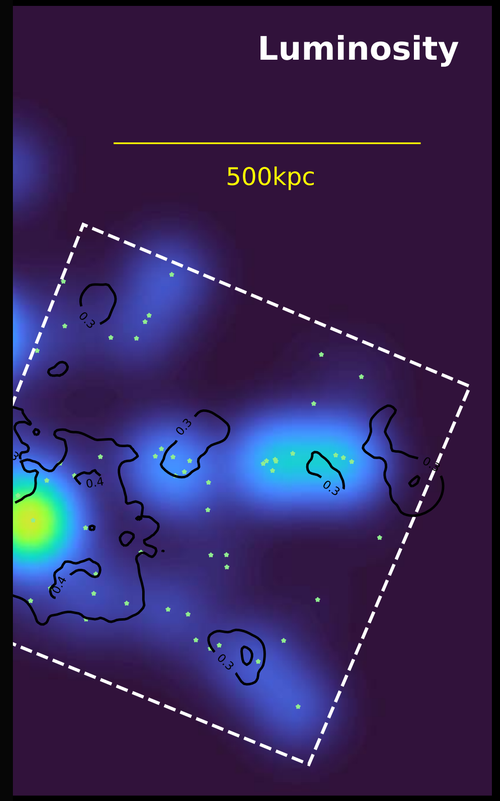
Refer to these two papers for more details on SNe analysis

Pascale et al. (including Cha) 2024; arXiv:2403.18902

Hubble constant inference

Mass map from MARS

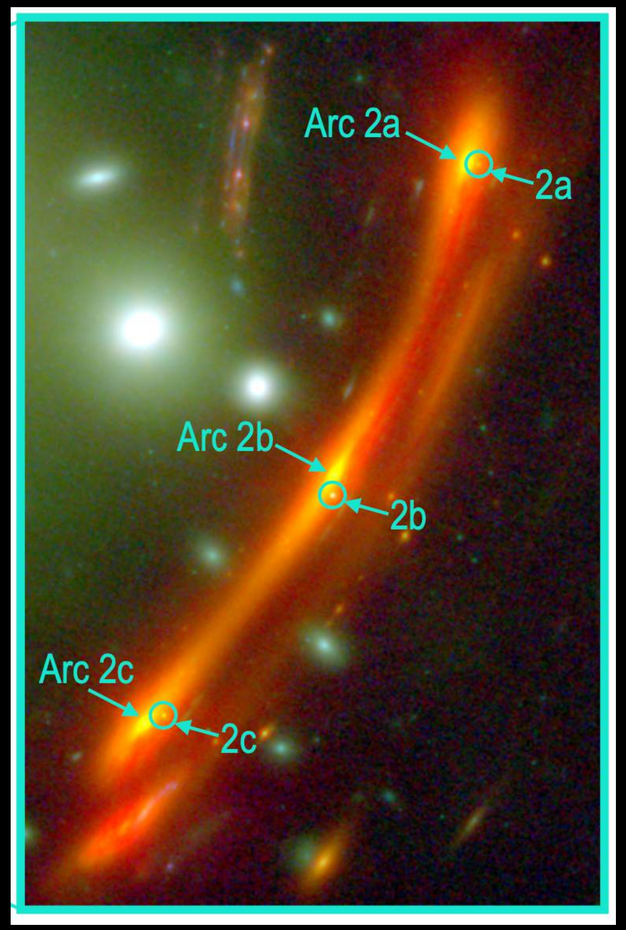


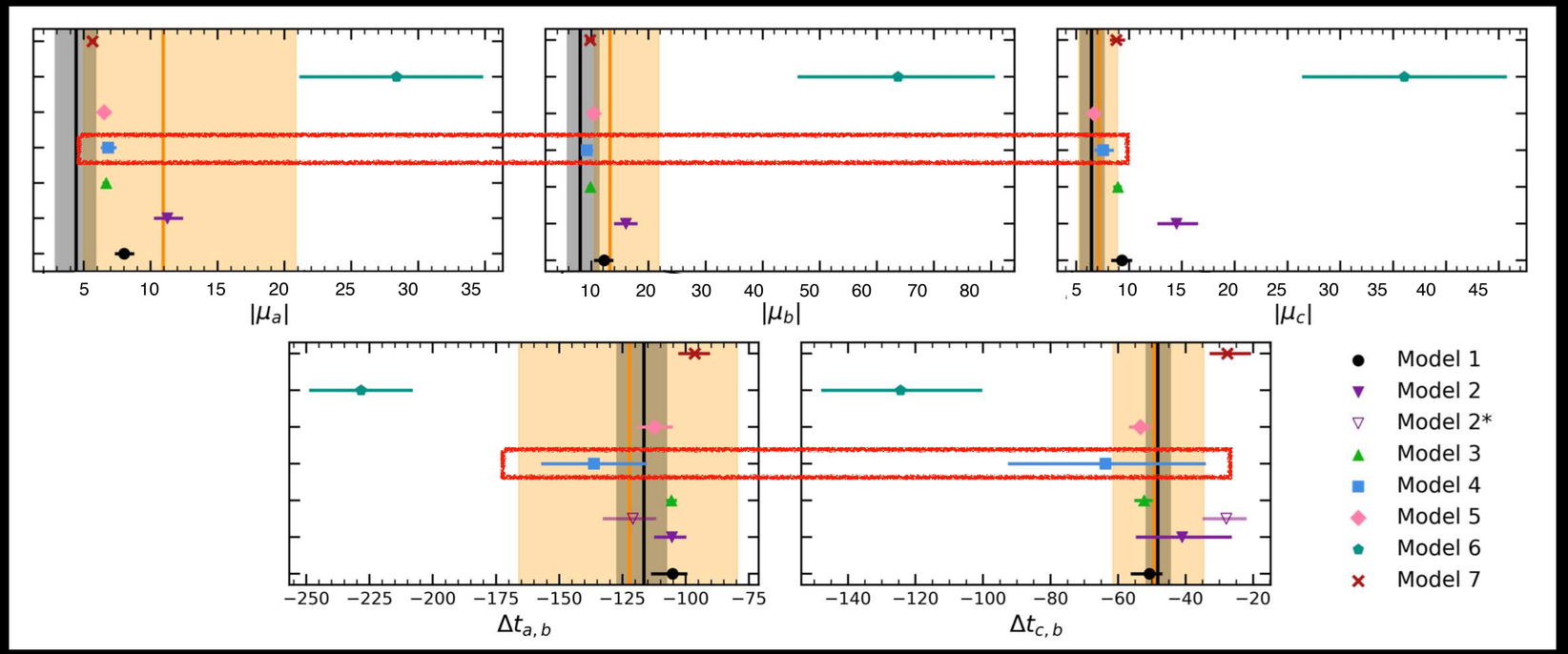


H_0 inference using SL

Reproducing ability

Model 4 is MARS





- Black: Measurement from photometric light curve fitting
- Orange: Measurement from spectroscopic age-dating
- Vertical lines & swaths: median and 68% confidence level

Pascale et al. (including Cha) 2024; arXiv:2403.18902

Hubble constant inference

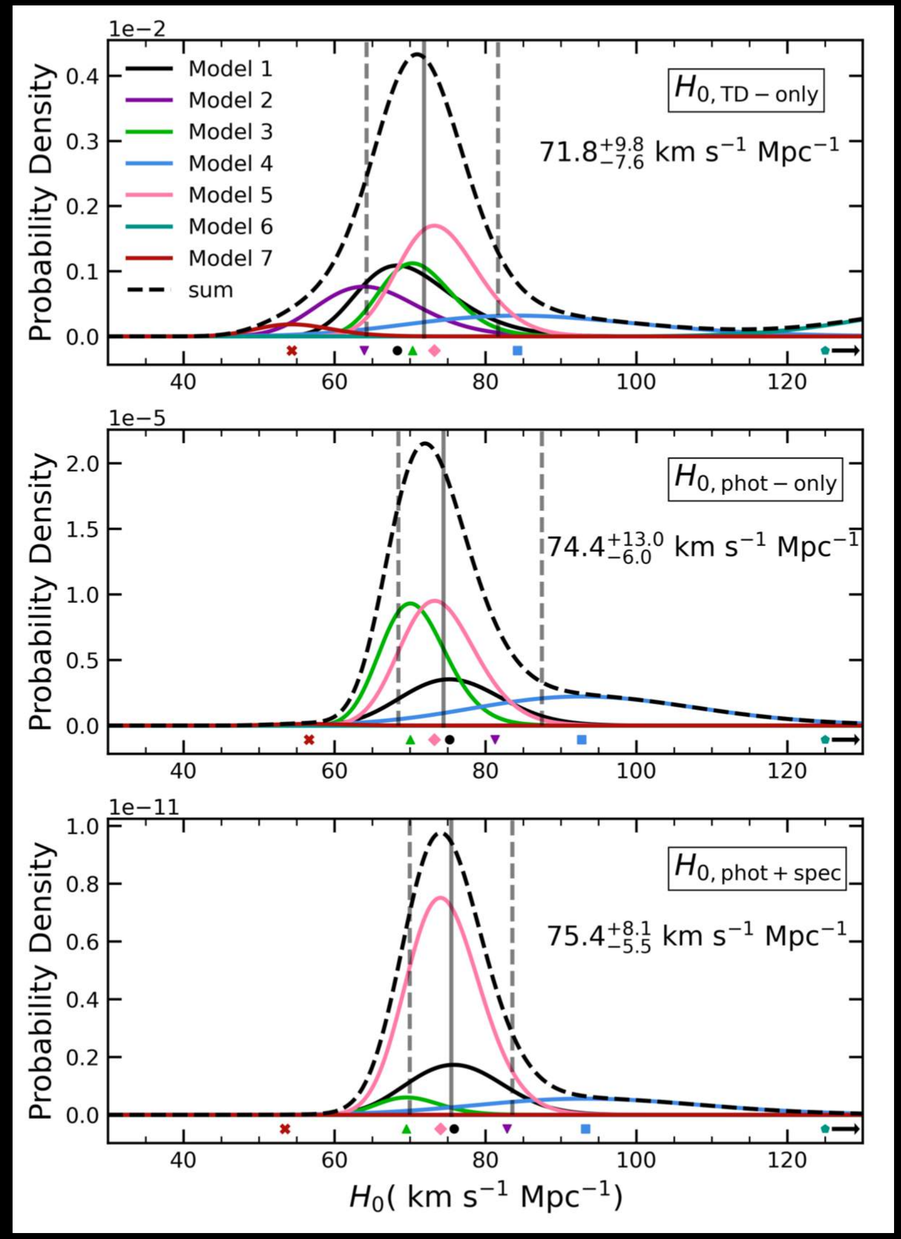
Combined Hubble constant

Table 2. H_0 Inferences

Lens Model	$H_{0,\mathrm{phot+spec}}$	$H_{0,\mathrm{phot-only}}$	$H_{0,\mathrm{TD-only}}$	$\mathrm{Weight}_{\mathrm{phot+spec}}$	$\mathrm{Weight}_{\mathrm{phot-only}}$	$\mathrm{Weight}_{\mathrm{TD-only}}$
1	$76.05^{+6.41}_{-6.01}$	$75.55^{+6.71}_{-6.31}$	$69.74^{+7.11}_{-5.81}$	0.19	0.16	0.21
2	$83.55^{+6.61}_{-5.91}$	$82.05^{+7.01}_{-6.11}$	$64.83^{+7.21}_{-6.41}$	0.00	0.00	0.16
3	$69.94^{+4.40}_{-3.90}$	$70.54^{+4.60}_{-4.10}$	$70.94^{+5.11}_{-4.50}$	0.04	0.28	0.16
4	$93.96^{+15.02}_{-14.31}$	$93.66^{+14.91}_{-14.21}$	$85.96^{+16.02}_{-14.21}$	0.14	0.22	0.15
5	$74.54^{+5.11}_{-4.70}$	$73.84^{+5.31}_{-4.80}$	$73.84^{+5.51}_{-5.01}$	0.63	0.33	0.27
6	> 130	> 130	> 130	0.00	0.00	0.03
7	$53.92^{+4.90}_{-4.40}$	$57.03^{+5.01}_{-4.50}$	$54.82^{+5.31}_{-4.80}$	0.00	0.00	0.03
Total	$75.4^{+8.1}_{-5.5}$	$74.4^{+13.0}_{-6.0}$	$71.8^{+9.8}_{-7.6}$	1.00	1.00	1.00

NOTE—The seven contributing cluster lens models with their individual predictions for the three H_0 (km s^{-1} Mpc^{-1}) inferences. Also listed are the relative weightings for each model in the likelihood across the three inferences. We also present the results for the total inference resulting from Eq. 5 and Eq. 7.

- Hubble constant inference performed by 3 different approaches.
  1. From time delay alone
  2. Including magnification
  3. Including spectroscopic constraints



Pascale et al. (including Cha) 2024; arXiv:2403.18902